U.S. DEPARTMENT OF COMMERCE
Alexander B. Trowbridge, Secretary

ENVIRONMENTAL SCIENCE SERVICES ADMINISTRATION
Robert M. White, Administrator

ENVIRONMENTAL DATA SERVICE
Woodrow C. Jacobs, Director

ESSA RESEARCH LABORATORIES

Solar-Geophysical Data

Descriptive Text

WASHINGTON, D.C.
FEBRUARY 1968

SOLAR - GEOPHYSICAL DATA

INTRODUCTION

This pamphlet contains the description and explanation of the data contained in the monthly publication "Solar-Geophysical Data", issued by the ESSA Research Laboratories of the Environmental Science Services Administration. The monthly bulletins are available on a data exchange basis through the World Data Center A, Upper Atmosphere Geophysics, ESSA, Boulder, Colorado 80302, or at a nominal cost through the U.S. Government Printing Office.* These data reports continue the series which were issued by the Central Radio Propagation Laboratory of the National Bureau of Standards, known since 1956 as the CRPL-F series Part B. The CRPL became the Institutes of Environmental Research in October 1965. The latter were reorganized as the ESSA Research Laboratories in November 1967. Since June 1965, the compilations and editing have been done by Miss Hope I. Leighton under the supervision of Miss J. Virginia Lincoln.

The reports are intended to keep research workers abreast of the major particulars of solar activity and the associated ionospheric, radio propagation and other geophysical effects. This report series is made possible through the cooperation of many observatories, laboratories and agencies as recorded in the detailed descriptions which follow.

Beginning with the February 1967 issue the data were regrouped within the reports and are being presented according to the month which the observations cover. The pink-paper section contains data for the month one month before the month of publication; the white-paper section contains data for the second month before; and the green-paper section contains data for the sixth month before the month of publication. Special data for miscellaneous times are given from time to time in the yellow-paper section. In this descriptive text the page colors correspond to those used for the data publication. These reports should not be considered as definitive publications because of the rapid publication schedule involved for the data from months one and two before that of publication. Errata or revisions are included from time to time. Additions to the descriptive text will appear with the data when new material is added, or revision is made.

The first page of each issue gives the general contents and is backed by a running index to locate data for a specific month for the past year. A complete index for data since July 1957 is given in the blue section of this text.

---

* For sale through the Superintendent of Documents, Government Printing Office, Washington, D. C., 20402. Subscription price: $8.75 annually for domestic mailing. Add $2.25 for foreign mailing. Single issue price 75 cents.

TABLE OF CONTENTS

DATA FOR ONE MONTH BEFORE MONTH OF PUBLICATION
TABLE OF CONTENTS

ALERT PERIODS

The table gives the Advance Geophysical Alerts as initiated by (or received by) the Western Hemisphere Regional Warning Center of the International Ursigram and World Days Service at Boulder, Colorado, and also the Worldwide Geophysical Alerts as designated by the IUWDS World Warning Agency, Boulder, Colorado.

These alerts are of the types recommended by the International Ursigram and World Days Service. A full description of the program can be found in IQSY NOTES No. 19, "1966-1967 World Days Program", which is available from the IUWDS Deputy Secretary, Miss J. Virginia Lincoln, ESSA, Boulder, Colorado, U.S.A. 80302. A revised program will be prepared during 1968. Pertinent information is given below:

Effective January 1, 1967 there were some changes in the scheme for the daily worldwide Alerts, the GEOALERTS. The new plan provides for GEOALERTS (also Advance Alerts, ADALERTS) to be covered by the following conditions (pp 8-9 of IQSY NOTES No. 19):

Solar Flares (in telegrams: SOFLARE). The GEOALERT statement distinguishes between occurrence of a really major flare (PROTONFLARE) and the existence of a region of flare activity (FLARES). Either kind may be forecast (EXPECTED), but only a PROTONFLARE will be recognized after its occurrence in the GEOALERT statement by giving date and time of its occurrence. In all cases, there will be given the heliographic position of the flare (at the time of occurrence) or of a flare-producing solar region (at 0400 UT on the date of the GEOALERT message); for example: "N25E62" for latitude North 25°, central meridian distance East 62°.

For ADALERTS, in addition to PROTONFLARE, the messages recognize all flares of numerical importance 2, 3, 4 and alphabetical importance B (bright), and all very outstanding radio solar noise bursts, especially at 10 cm wavelength, and those of Type IV.

Magnetic Storms (in telegrams: MAGSTORM). The GEOALERT statement attempts to mark the major magnetic disturbances either in a forecast (EXPECTED) or by recognition (EXISTS, or date and time of commencement). As appropriate, self-explanatory words like GREAT, MAJOR, AURORA, will be appended. In general, the ADALERT statement will only recognize the commencement of a storm rather than make forecasts.

Cosmic Events (in telegrams: COSMIC EVENT). The GEOALERT message recognizes a major change in the level of cosmic-ray flux as seen by a neutron monitor, such as FORBUSH DECREASE EXISTS; or COSRAY INCREASE with date and nominal time if available. Also a significant PCA event will be identified by POLCAP ABSORPTION EXISTS. The same conditions are suitable for ADALERT statements.

Stratospheric Warming Alert. These are distributed along with the GEOALERT message but will be identified separately as STRATWARM Alerts.

D A I L Y S O L A R I N D I C E S

The first table presents Zürich relative sunspot numbers, R_Z, for the month. The corresponding data for eleven earlier months are reprinted to permit the trend of solar activity to be followed. On the same page is presented a similar table of twelve months of daily solar flux values at 2800 MHz adjusted to one Astronomical Unit, S_a, as reported by the Algonquin Radio Observatory (ARO) of the National Research Council near Ottawa.

The next table gives several available daily indices for the month preceding that of publication. In addition to the calendar date, the table gives the day-number of the year and the day-number of the standard 27-day (solar rotation) cycle. The data presented are Zürich relative sunspot numbers, (R_Z), American relative sunspot numbers, (R_A'), daily solar flux values at 2800 MHz, (S), and daily solar flux values, (S_a), adjusted to 1 A.U. for 8800, 4995, 2800, 2695, 1415, and 606 MHz.

Graph of Sunspot Cycle -- A graph illustrates the recent trend of Cycle 20 of the 11-year sunspot cycle with predictions of the future level of activity. The customary "12-month" smoothed index, R_{12}, is used throughout, the data being final R_Z numbers except for the current year.

$$R_{12} = 1/12 \sum_{n-5}^{n+5} \left[R_k + 1/2\ (R_{n+6} + R_{n-6})\right]$$ in which R_k is the mean value of R for a single month k and R_{12} is the smoothed index for the month represented by k = n. Predictions shown are those made for one year after the latest available datum by the method

of A. G. McNish and J. V. Lincoln (Trans. Am. Geophys. Union, 30, 673-685, 1949) modified by the use of regression coefficients and mean cycle values recomputed for Cycles 1 through 19. Cycle 20 began October 1964, when the minimum $\bar{R}$ of 9.6 was reached. The values of the smoothed index, R, are given in a table following the graph. They also appear regularly in the Ionospheric Telecommunications Laboratory's "Ionospheric Data" reports and "Ionospheric Predictions" series.

Relative Sunspot Numbers -- The relative sunspot number is an index of the activity of the entire visible disk of the sun. It is determined each day without reference to preceding days. Each isolated cluster of sunspots is termed a sunspot group and it may consist of one or a large number of distinct spots whose size can range from 10 or more square degrees of the solar surface down to the limit of resolution (e.g. 1/25 square degree). The relative sunspot number is defined as $R = K(10g + s)$, where g is the number of sunspot groups and s is the total number of distinct spots. The scale factor K (usually less than unity) depends on the observer and is intended to effect the conversion to the scale originated by Wolf. The provisional daily Zürich relative sunspot numbers, R_Z, based upon observations made at Zürich and its two branch stations in Arosa and Locarno are communicated by M. Waldmeier of the Swiss Federal Observatory. The daily American relative sunspot numbers, R_A', are compiled by Richard H. Davis, Boston, Massachusetts, for the Solar Division of the American Association of Variable Star Observers. The R_A' observations for sunspot numbers are made by a rather small group of extraordinarily faithful observers, many of them amateurs, each with many years of experience. The counts are made visually with small, suitably protected telescopes.

Final values of R_Z appear in the IAU Quarterly Bulletin on Solar Activity, the Journal of Geophysical Research, these reports, and elsewhere. They usually differ slightly from the provisional values. The American numbers, R_A', are not revised.

Daily Solar Flux Values - Ottawa-ARO -- Daily observations of intensities of the 2800 MHz radio emission which originates from the solar disk and from any active regions present are made at the Algonquin Radio Observatory (ARO) of the National Research Council near Ottawa with a reflector 1.8 meters diameter as a continuation of observations which commenced in Ottawa in 1947. Entries refer to a single calibration made near local noon at 1700 UT. When the flux changes rapidly, or there is a burst in progress, the reported value is the best estimate of the undisturbed level for the whole observing day. The various types of outstanding events are listed separately in another table. The observed flux values have

variations resulting from the eccentric orbit of the earth in its annual path around the sun. Although these radio values are suitable to use with observed ionospheric and other data, an adjustment must be introduced when the observations are used in studies of the absolute or intrinsic variation of the solar radio flux. Thus the tables show both the observed flux S, and the flux adjusted to 1 A.U., S_a. A graph showing the monthly highs and lows for the last two sunspot cycles is shown in this text. Relative errors over long periods of time are believed to be about $\pm 2\%$, over a few days may be $\pm 0.5\%$. Measurements made with a calibrated horn antenna during the fall of 1967 indicate that the monthly mean values of daily flux observed on the I.T.U. allocation of 2695 MHz are 3% lower in relation to values observed on corresponding days on the frequency of 2800 MHz. Examination of the relative ratio of the flux observed at DRAO on 2695 MHz to the 2800 MHz flux observed at ARO have shown a downward trend since the beginning of the present sunspot cycle amounting to about 3%, superimposed upon accidental variations of the same magnitude. Absolute measurements of solar fluxes as recommended by Commission 5 of URSI are still in progress. A discussion of the absolute errors in the intensity measurements was presented to the XVth General Assembly of URSI by H. Tanaka and T. Kakimura (Information Bulletin of Solar Radio Observatories, No. 21, page 6, November 1966).

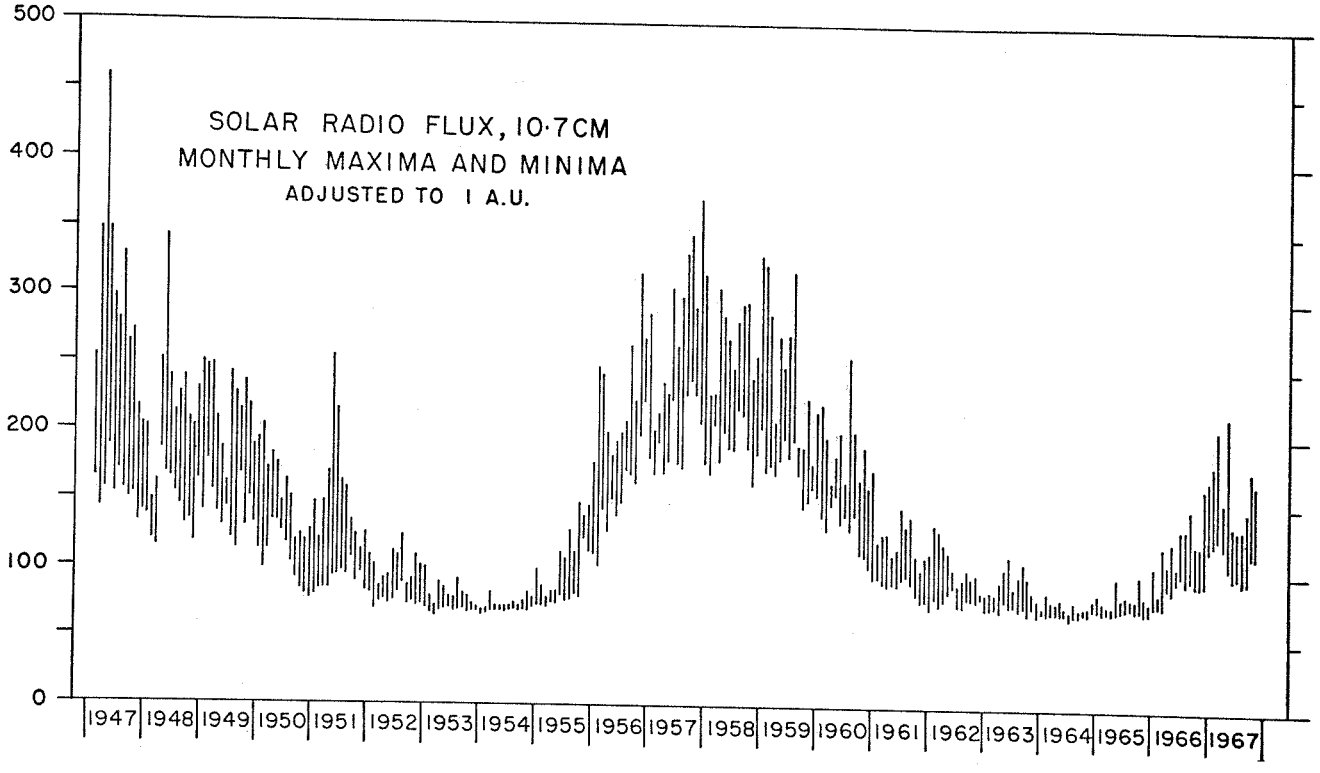

Commencing in 1966, a correction for atmospheric attenuation due to the variable zenith angle of the sun was incorporated in the reported daily flux levels. In order to minimize the discontinuity

between current tabulations and past tabulation in which the absorption correction was neglected, the correction factor was separated into two parts: a constant part corresponding to a fixed loss when the sun is at the "zenith distance" of summer solstice and a variable part corresponding to the difference in loss between summer solstice and when the sun is at greater zenith distances during other times of the year. The constant correction given by a multiplier of 1.011 is not incorporated into the tabulations for 1966 onwards and so must be considered as an alteration to the listed absolute values of solar flux. The variable multiplier has been included in the flux values as listed; it has values given by the table:

January	1.015	July	1.000
February	1.009	August	1.001
March	1.004	September	1.003
April	1.002	October	1.007
May	1.001	November	1.012
June	1.000	December	1.017

These solar radio noise indices are being published in accordance with a CCIR Recommendation originally from the Xth Plenary Assembly, Geneva, 1963 (and maintained at Oslo, 1966), which states "that the monthly-mean value of solar radio-noise flux at wavelengths near 10 cm should be adopted as the index to be used for predicting monthly median values of foE and foF1, for dates certainly up to 6, and perhaps up to 12 months ahead of the date of the last observed value of solar radio-noise flux".

Daily Solar Flux Values - AFCRL Sagamore Hill -- The Sagamore Hill Solar Radio Observatory of the Air Force Cambridge Research Laboratories (located at 42°37'54"N, 70°49'15.15"W) in 1966 began operating solar patrols at 8800, 4995, 2695, 1415, and 606 MHz. Flux calibrations are made at about meridian transit each day. All flux data are corrected to sun-earth distance of 1 A.U. Corrections are also made for atmospheric attentuation based on the following average vertical attentuations:

8800 MHz	0.0777 db	1415 MHz	0.0555 db
4995	0.06105	606	0.04995
2695	0.05661		

SOLAR CENTERS OF ACTIVITY

Calcium Plage and Sunspot Regions -- This table gives particulars of the centers of activity visible on the solar disk during the preceding month. These are based on estimates made and reported on the day of observation and are therefore of limited reliability. The calcium plage region identifications, in particular, should be considered preliminary, subject to change after more detailed scrutiny.

The table gives the heliographic coordinates of each calcium plage center in terms of the Greenwich date of passage of the sun's central meridian (CMP) and the latitude; the serial number of the plage as assigned by McMath-Hulbert Observatory: the serial number of the center in the previous solar rotation, if it is a persisting region, or an otherwise appropriate statement; particulars of the plage at CMP: area, central intensity; a summary of the development of the plage during the current transit of the disk, where b = born on disk, L = passed to or from invisible hemisphere, d = died on disk, and / = increasing, - = stable, \ = decreasing; age in solar rotations; date first seen, month/day; and duration of plage on disk given in days; particulars of the associated sunspot group, if any, at CMP: area and spot count and the summary of development during the current disk transit, similar to the above together with Mt. Wilson number. The unit of area is a millionth of the area of a solar hemisphere; the central intensity of the calcium plages is roughly estimated on a scale of 1 = faint to 5 = very bright and refers to the brightest part of the plage. Parentheses indicate region was not observed on CMP date; values are those nearest CMP date.

Calcium plage data are available through the cooperation of the McMath-Hulbert Observatory of the University of Michigan under ESSA contract. The sunspot data are compiled from reports from the Sacramento Peak Observatory and ESSA-Boulder as well as reports received through the network of the International Ursigram and World Days Service.

Magnetic Classifications of Sunspots -- This table lists the date and time (UT) of the observations, the approximate heliocentric coordinates, the magnetic classification of the sunspot groups together with the largest magnetic field strength measured in the group and the group number, as observed at the Mount Wilson Observatory. This is the group number of the series which used to be published in the Publications of the Astronomical Society of the Pacific. The magnetic classifications are defined as follows:

αp All the magnetic measures in the group are of the same polarity which is that corresponding to the preceding spots in that hemisphere for that cycle.

αf All the magnetic measures in the group are of the same polarity which is that corresponding to the following spots in that hemisphere for that cycle.

βp A bipolar group in which the magnetic measures indicate that the preceding spots are dominant.

β A bipolar group in which the magnetic measures indicate a balance between the preceding and following spots.

βf A bipolar group in which the magnetic measures indicate that the following spots are dominant.

$\beta\gamma$ A group which has general β characteristics but in which one or more spots are out of place as far as the polarities are concerned.

γ A group in which the polarities are completely mixed.

Statements will be added to the above classifications if the group is also of the "δ-configuration": spots of opposite polarity within 2° of one another and in the same penumbra.

Starting with data for July 1966 these Mount Wilson magnetic sunspot classification lists include the Mount Wilson serial numbers for all spot groups observed at Mount Wilson. If a magnetic classification is based on magnetic measurements, that classification is enclosed in parentheses. A magnetic classification not enclosed in parentheses is determined from the appearance of the spot groups and the plage. An "X" in the classification column indicates sufficient information was not available to make an intelligent determination of the magnetic classification. Prior to July 1966 the only magnetic classifications included in the lists were those for which there were magnetic measurements.

The largest magnetic field strength measured in each group is now given. Starting with the data for August 1966, the number which appears on the right-hand side of the column labeled "Type" is a coded representation of the largest magnetic field strength

measured in the group. The field strength is only given to the nearest 500 gauss because it is felt that the uncertainties of measurement do not permit more than that accuracy. These measurements are made with the line λ5250.216 (Fe I). No correction is made for blending of the Zeeman components. The code is as follows:

Code	Maximum Field Strength in Gauss
1	100-500
2	600-1000
3	1100-1500
4	1600-2000
5	2100-2500
6	2600-3000
7	3100-3500
8	3600-4000
9	4100-4500
10	>4500

SOLAR FLARES

The solar flare data from the month before that of publication are divided into two tables. The first table is restricted to the record of solar flares for which one or more observatories assigned a numerical importance of "1" or greater.* The heading is marked PARTIAL to emphasize these reports are those received at ESSA on a rapid schedule. To make the report of occurrence of flares more comprehensive, the flares reported only as subflares are listed in the second table by time of beginning in UT and coordinates only. In the section of these bulletins presenting data for the sixth month before that of publication, verification of questionable values has been attempted, and the heading is "Original Reports and Statistical Summaries".

The solar flare reports are received from throughout the world at World Data Center A, Upper Atmosphere Geophysics, Boulder, Colorado. Observations are made in the light of the center of the Hα line unless noted otherwise. The reports from Sacramento Peak, New Mexico are from observations at the USAF Sacramento Peak Observatory at Sunspot, New Mexico. ESSA operates the flare patrol at Boulder, and ESSA contracts support the flare patrols at McMath-Hulbert, Culgoora, and the Swedish Astrophysical Station on Capri. Haleakala observations are made in conjunction with NASA-supported Solar Research Programs. Canary and Carnarvon are supported jointly by ESSA and NASA funds.

---

* The complete provisional listings can be made available at cost through the World Data Center A, Upper Atmosphere Geophysics, ESSA, Boulder, Colorado U.S.A. 80302.

The columns in the table are as follows:

-reporting observatory using IAU Quarterly Bulletin on Solar Activity designations;
-the universal date;
-beginning and ending times in UT;
-time of maximum phase in UT;
-the heliographic coordinates in degrees for the "center of gravity" of the emission region, corresponding to the time of maximum intensity;
-the distance from center of disk in units of the disk radius;
-McMath serial number of the associated plage region;
-the time of central meridian passage of the position of the flare in tenths of the Universal date;
-duration in minutes;
-the flare importance on the IAU scale of Sf* to 4b (see below);
-observing conditions where 1 means poor, 2 fair and 3 good;
-nature and completeness of available observations where

C** = a complete, or quasi complete sequence of photographs was obtained,
P** = one or a few photographs of the event were obtained resulting in incomplete time coverage,
V = all (or most of) the development of the flare was visually observed, or
S = flare was seen visually for a small part of its probable duration;

-time of measurement for either tabulated width of Hα to nearest 1/10A or for tabulated area;
-measured (i.e. projected) area at maximum intensity in heliographic square degrees (reported originally in millionths of disk by observatory) -- this is not necessarily the maximum area;
-corrected area in square degrees (see below);
-maximum effective line-width in Hα to nearest 1/10A;
-maximum intensity expressed in percent of the local continuum;
-and remarks in the IAU system of notes where

A = Eruptive prominence, base at >90°.
B = Probably the end of a more important flare.
C = Invisible 10 minutes before.
D = Brilliant point.
E = Two or more brilliant points.
F = Several eruptive centers.
G = No spots visible in the neighborhood.
H = Flare with high velocity dark surge.
I = Very extensive active region.
J = Plage with flare shows marked intensity variations.
K = Several intensity maxima.
L = Filaments show effects of sudden activation.
M = White-light flare.
N = Continuous spectrum shows effects of polarization.
O = Observations have been made in the calcium II lines H or K
P = Flare shows helium D_3 in emission.
Q = Flare shows the Balmer continuum in emission.
R = Marked asymmetry in Hα line.
S = Brightening follows disappearance of filament (same position).
T = Region active all day.
U = Close and somewhat parallel bright filaments (|| or Y shape).
V = Occurrence of an explosive phase.
W = Great increase in area after time of maximum intensity.
X = Unusually wide Hα emission.
Y = Onset of a system of loop-type prominences.
Z = Major sunspot umbra covered by flare.

---

* For easier visual selection of the more important flares a minus sign, "-", is used to indicate subflares instead of "S".

** Circumstances C and P can occur with any type of photographic patrol, whether automatic or not. Combinations of two symbols can be used for intermediate circumstances, example: VP = continuous visual watch plus a few photographs.

The following symbols are used in the table to explain accuracy of the times reported:

D = greater than
E = less than
U = approximate

All times are Universal Time (UT or GCT).

The no-flare patrol observations matching the solar flare table are given in graphical form. The observatories reporting the patrols are indicated. The darker area on the graph are times of no cinematographic or visual patrol. The rest of the shaded areas are times of visual, but no cinematographic patrol.

The new dual importance scheme, adopted January 1, 1966 by IAU Commission 10, is summarized in the following table:

"Corrected" area in square degrees	Relative Intensity Evaluation		
	Faint (f)	Normal (n)	Brilliant (b)
≤2.0	Sf	Sn	Sb
2.1 - 5.1	1f	1n	1b
5.2 - 12.4	2f	2n	2b
12.5 - 24.7	3f	3n	3b
>24.7	4f	4n	4b

The area to be used in assigning the first figure of the dual importance, is the area of the flaring region at the time of maximum brightness. The observatory measures apparent area in millionths of the solar disk. For flares less than 65° from the center of the solar disk, the formula relating apparent and corrected area is:

$$\text{"corrected" area} = \frac{\text{apparent area}}{97} \times \sec\theta$$

where apparent area is in millionths of the disk and corrected area is in heliographic square degrees.

For flares more than 65° from the center, the "sec θ law" becomes unsatisfactory. The first importance figure can be estimated from the table below where areas are given in millionths of the disk.

Angle	0°	------	65°	70°	80°	90°
Limit S-1	200	sec θ law	90	75	50	45
Limit 1-2	500	sec θ law	280	240	180	170
Limit 2-3	1200	sec θ law	600	500	350	300

The intensity scale shown as the second importance figure is only a qualitative one where each observatory uses its experience to decide if a flare is rather faint (f), normal (n), or rather bright (b).

SOLAR FLARE OBSERVATORIES

CODE NO.	OBS. TYPE	I. A. U. ABREV.	NAME, PLACE AND COUNTRY
824	C	ABST	ABASTUMANI,GEORGIAN,SSR
512	VP	ARCE	ARCETRI,FLORENCE,ITALY
521	VP	AROS	AROSA,SWITZERLAND
508	VP	ATHN	NATL OBS,ATHENS,GREECE
832	C	BAKO	BAKOU,PIRCULI,USSR
647	C	BOUL	BOULDER,COLORADO,USA
560	C	BUCA	NATL OBS,BUCHAREST,ROMANIA
557	C	CANA	GRAN CANARIA,CANARY ISLANDS
506	VP	CAPF	ANACAPRI,ITALY(GERMAN)
519	V	CAPS	ANACAPRI,ITALY(SWEDISH)
570	VP	CATA	CATANIA,SICILY,ITALY
639	C	CLMX	HIGH ALTITUDE OBS,CLIMAX,COLORADO,USA
826	C	CRIM	SIMEIS,CRIMEA,RSFSR
403	C	CRON	CARNARVON,AUSTRALIA
402	C	CULG	CULGOORA,AUSTRALIA
478	C	HALE	HALEAKALA,MAUI,HAWAII,USA
537	VP	HERS	R.GREENWICH OBS,HERSTMONCEUX,ENGLAND
646	C	HOUS	HOUSTON,TEXAS,USA
718	C	HUAN	GEOPHYSICAL INST,HUANCAYO,PERU
313	V	IKOM	IKOMASAN OBS,KYOTO,JAPAN
358		ISTA	UNIV.OBS,ISTANBOUL,TURKEY
382	VP	KAND	KANDILLI OBS.,ISTANBOUL,TURKEY
547	V	KANZ	GRAZ OBS,KANZELHOHE,AUSTRIA
827	VP	KHAR	KHARKOV,UKRANIAN,SSR
828	C	KIEV	KIEV,GAO,UKRANIAN,SSR
309	VP	KODA	KODAIKANAL,INDIA
522	VP	LOCA	LOCARNO,SWITZERLAND
659	C	LOCK	LOCKHEED,LOS ANGELES,CALIFORNIA,USA
876	VP	LVOV	LVOV,UKRANIAN,SSR
468	VP	MANI	MANILA,PHILIPPINE ISLANDS
642	C	MCMA	MCMATH-HULBERT,PONTIAC,MICHIGAN,USA
505	C	MEUD	MEUDON,FRANCE
314	C	MITK	MITAKA,TOKYO,JAPAN
555	C	MONT	MONTE MARIO OBS,ROME,ITALY
515		NERA	NEDERHORST DEN BERG,NETHERLANDS
504	V	ONDR	ONDREJOV,PRAGUE,CZECHOSLOVIA
603	C	OTTA	OTTAWA,ONTARIO,CANADA
359		PURP	PURPLE MTN,NANKING,CHINA
645	C	SACP	SACRAMENTO PEAK,SUNSPOT,NEW MEXICO,USA
572	VP	SALO	SALONIQUE(THESSALONIKA)GREECE
520		SALT	SALTSJOBADEN,STOCKHOLM,SWEDEN
758	C	SANM	SAN MIGUEL,ARGENTINA
862	VP	SIBE	SIBERIE(SIBERIAN IZMIR)IRKUTSK,RSFSR
833	C	TACH	TACHKENT,UZBECK,SSR
556	C	TORT	TORTOSA,SPAIN
502	C	UCCL	UCCLE,R.O.BRUSSELS,BELGIUM
834	C	VORO	VOROSHILOV,USSR
546	VP	WEND	WENDELSTEIN,GFR
523	VP	ZURI	EIDGENOSSISCHE STERNWARTE,ZURICH,SWITZERLAND

The table on page 15 gives the solar flare observatories presently cooperating in international data interchange through the World Data Centers originally established during the International Geophysical Year. For each observatory are given the code numbers used on the punched cards at ESSA; the four letter IAU abbreviations; name, place and country; and type of patrol where C, V and P have the meanings explained above.

Note: All the flare data are recorded on punched cards. As errata are received the punched cards are corrected. These errata are not always published in these reports. Copies of the cards, tabulations from them or some data on magnetic tape are available at cost through the World Data Center A Upper Atmosphere Geophysics, ESSA, Boulder, Colorado U.S.A 80302.

SOLAR RADIO WAVES

Outstanding Occurrences -- Beginning with data for October 1966 the outstanding occurrences from western hemisphere stations observed at discrete frequencies were combined together and presented in one table. They now appear for the month before that of publication. The discussions below give the reporting details for each individual reporter.

In the table a single solar event is indicated by brackets. The observing station is given followed by type of event. For each event start and maximum phase in UT, duration in minutes and peak and mean flux densities in $10^{-22} Wm^{-2} Hz^{-1}$ are listed. From time to time illustrations of selected outstanding bursts will be included.

The table which follows gives the key for identifying type of event. The name code used to identify each reporting station and the frequencies reported by each station appear in a second table.

1 = Simple 1	22 = Simple 3F	40 = Fluctuations
2 = Simple 1F	23 = Simple 3AF	41 = Group of Bursts
3 = Simple 2	24 = Rise	42 = Series of Bursts
4 = Simple 2F	25 = Rise A	43 = Onset of Noise Storm
5 = Simple	26 = Fall	44 = Noise Storm in Progress
6 = Minor	27 = Rise and Fall	45 = Complex
7 = Minor +	28 = Precursor	46 = Complex F
8 = Spike	29 = Post Burst Increase	47 = Great Burst
20 = Simple 3	30 = Post Burst Increase A	48 = Major
21 = Simple 3A	31 = Post Burst Decrease	49 = Major +
	32 = Absorption	

Code	Station	Frequencies Reported, MHz
BOUL	Univ. of Colorado - Boulder	18
BOUL	ESSA - Boulder	184
HALE	Haleakala - Hawaii	107, 18
MCMA	McMath-Hulbert - Michigan	18
OTTA	ARO - Ottawa	2800
PENN	Pennsylvania State Univ.	10700, 2690, 960, 328
PENT	DRAO - Penticton	2695
SANM	San Miguel, Argentina	408
SAOP	Sao Paulo, Brazil	7000
SGMR	AFCRL - Sagamore Hill	15400, 8800, 4995, 2695, 1415, 606
WASH	Washington State Univ.	486

Details of Observatories -- 2800 MHz Ottawa ARO and 2695 MHz Penticton - (DRAO) -- Enhancements of the solar radio flux from a slowly varying or a constant level during the day are listed separately as outstanding events or bursts on the basis of the classification described by Covington in Jour. Royal Astro. Soc. Can. 45, 1951, and Paper 28, Paris Symposium on Radio Astronomy 1959. The events are from the Algonquin Radio Observatory (45°57'N, 78°03'W) and from the Dominion Radio Astrophysical Observatory (DRAO) at Penticton, B.C. (49°19'N, 119°37'W). From the beginning, the solar radio noise enhancements at 2800 MHz have been described by type names that are indicative of the general structure found from visual inspection of the records as well as by numerical values of maximum burst intensity and duration. It has been found that these types also have application for bursts observed throughout the microwave region. Recent records of solar noise bursts observed simultaneously at the two widely separated stations of A.R.O. and D.R.A.O. have lead to the recognition of new variations which are sufficiently unique to be regarded as new types of bursts. Even though these events occur infrequently, they are needed in any morphological description of burst profiles and are probably associated with unique physical processes in the solar atmosphere. A summary of the burst types in use at the end of 1966 is provided on page 18. The numbers assigned by the URANE code of the International Ursigram and World Days Service for those events known at the time IGY are indicated in small circles.

The peak intensity of the microwave event ranges from a threshold value of 1 to 3 flux units to several thousand flux units, while the duration varies from a fraction of a minute to several hours. The threshold level depends upon such factors as residual receiver noise and the interference patterns produced at sunrise and sunset by the direct solar ray and one reflected from the earth. Most of the microwave events are single events with various flux variations or profiles. A large proportion show a simple smooth rise to a single peak followed by a slow decay to the pre-existing undisturbed flux level. When the intensity and duration of single-simple bursts are plotted in a graph, a two pronged scatter of points is found. This may be numerically described by three regions designated as regions 1, 2 and 3 and corresponding numbers assigned to the bursts. Simple 1 bursts have intensities less than 10 flux units and durations between 1 minute and 10 minutes (previous to Jan. 1968 the limit was set at 7-1/2 flux units and 7-1/2 minutes). Simple 2 bursts have intensities greater than 10 flux units and durations ranging from 1 minute to 60 minutes depending upon the intensity. Simple 3 bursts have durations in the range from 10 minutes to several hours but with intensities seldom exceeding 50 flux units. Visual inspection of the records immediately suggests "Impulsive Burst" for describing the Simple 2 burst and "Long Enduring Burst" for the Simple 3 event. Bursts with duration less than 1 minute and with intensity much greater than the threshold noise are termed Spikes.

Single bursts with two or more prominent peaks also fall into the numerical categories outlined for the simple bursts. Such bursts with duration and intensity similar to the Simple 2 bursts are termed "Complex Bursts", while bursts with parameters similar to the Simple 3 burst are still designated as Simple 3 events. In both cases, the time of commencement and peak intensity of the various components are described under the entry of Components.

When a number of single bursts occur in succession and the flux level returns to the steady pre-burst level for each event and remains there for durations ranging from a few minutes to several burst durations, the composite event is termed a "Group". The number of individual bursts is given, the maximum intensity of one event and the overall duration. Individual events are described as usual.

Irregularities observed in the otherwise smooth or gradual changes in a simple or complex burst are ripples, small rapid fluctuations and spikes. These are described as "Fluctuations"; they are not given any numerical values but their presence is indicated by the addition of the letter "F" to the main descriptive term. Components of complex bursts are regarded as "fluctuations" when the intensity is less than 15% of the main peak. Any structure of bursts in region 1 is also designated by "F" when not severely masked by the variations of the threshold.

When the complexity of a small burst is such that it is difficult to tabulate individual parts, or many rapid fluctuations blur the otherwise smooth variation of a simple or complex burst, the event is termed a "Period of Irregular Activity".

A gradual increase in flux preceding a more intense burst is designated as a "Precursor" while an enhanced level following a burst is designated a "Post Burst Increase". These may occur separately with bursts or in association with one another with respect to a more intense burst. When the precursor and post-burst increase have the same intensity, or may be smoothly joined together, the two features are combined into a "simple type 3" burst. This type of event is designated by the letter "A". The superposition of bursts with different durations, one on top of the other, can thus be tabulated. In each case, individual component intensities of single bursts are measured and listed separately.

A moderate rise of flux from 5 to 30 minutes duration with no accompanying decline during the following hours is designated as a "Rise Only". Gradual rises of greater duration are automatically considered in the calibration levels made every three hours. A similar description holds for the "Fall Only".

Microwave bursts with intensity greater than 500 flux units are of special geophysical interest but occur infrequently. They are described as "Great Bursts". The profiles generally exhibit great complexity: there may be an early, short duration impulsive burst followed by a second impulsive burst of comparable intensity but of greater duration. In the URANE code these great bursts are listed as Complex Bursts.

The types of bursts discussed all indicate an increase in radio emission from the sun and form the majority of events observed in the microwave region. The first clear indication of absorption occurred on May 19, 1951 as a "Post Burst Decrease" after the occurrence of an impulsive burst. The first clear indication of absorption alone occurred twice on June 20, 1967 and was recorded simultaneously at A.R.O. and D.R.A.O.

The burst peak intensity is measured in flux units without any adjustment for the varying sun-earth distance. For the smaller bursts, the errors in intensity will be only slightly greater than those entering into the calibration and estimated as ±5%. For the more intense bursts, the errors are estimated as ±15%. The continuous intensity scale may be replaced by using the following 9 flux intervals; below 1 unit, 1-9, 10-49, 50-99, 100-499, 500-999, 1000-2499, 2500-4999, and above 5000 (Harvey Astrophy. J. 139, 16-44, 1964). Mean flux is estimated or calculated using the listed intensity and duration and the actual burst profile for each event.

The commencement of a burst is taken when the enhancement of the flux shows a departure from the steady level of approximately 1 flux unit. For many of the bursts, this may be determined to within a few seconds with the exception of some of the long enduring bursts which have been described as "Gradual Rise and Fall" bursts. For these the uncertainty in determining the start may be as great as 5 minutes. The letter "E" appearing after the time of start indicates that the burst was already in progress at this time. Profiles of typical bursts are produced below.

MICROWAVE BURST TYPES - 2695 MC/S - OTTAWA, CANADA

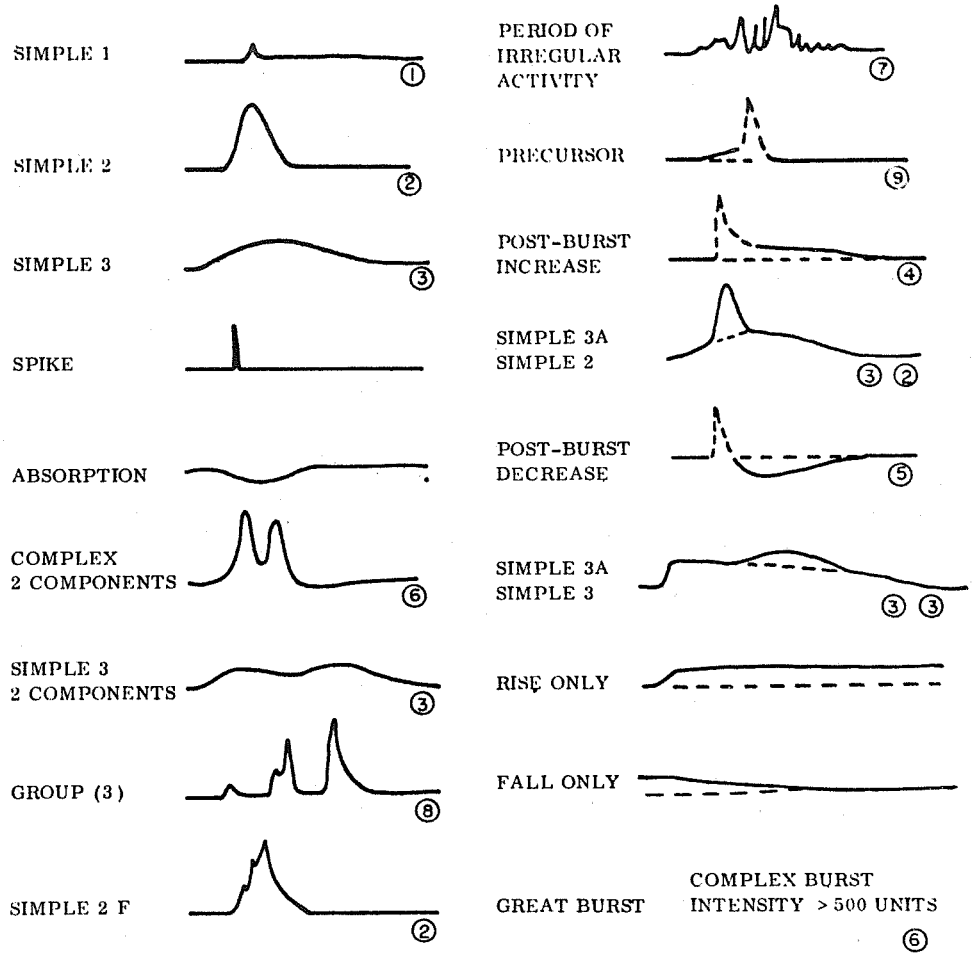

7000 MHz - Mackenzie University, Sao Paulo, Brazil -- Continuous radio observations of the sun have been made at Umuarama Radio Observatory (22°46'S, $3^h02.5^m$W) by Mackenzie's Radio Astronomy Group, at the frequency of 7000 MHz, since March 1967. The equipment was described in Mackenzie University Annual Report GRAM-23 (January 1967). It consists of a polarimeter with a 1.5m paraboloidal reflector on an equatorial mount, presenting minimum detectable temperature near 1°K being capable to measure overall solar circular polarization when its degree is above 0.3%. The period of observation is approximately from 10^h00^m UT to 19^h00^m UT, and the daily mean values of flux and polarization are averaged during this period and then corrected to 1 A.U. The bursts recorded are classified following the Covington method (J. Astron. Soc. Canada 45, 1951) as shown on page 18. Details of bursts as for their polarization features are also available, such as their degree of polarization, variability and relationships with the total flux features.

The system uses a square law detector and the reference levels are the empty sky temperature and a matched load temperature (at ambient temperature). A final calibration check is done by comparing the 7000 MHz data with spectral values obtained from undisturbed sun observations performed at neighbouring frequencies by AFCRL Sagamore-Hill Observatory, and by Nagoya University's Toyokawa Radio Observatory.

10700, 2700, 960 and 328 MHz Pennsylvania State University -- The Radio Astronomy Observatory at the Pennsylvania State University is conducting a daily solar patrol at 10,700, 2700, 960 and 328 MHz. An interferometer operating at 108 MHz has been completed and is being tested. The purpose of this patrol is to obtain correlated flux measurements with emphasis on solar bursts.

The antennas for the four radiometers now operating are all mounted on a single polar tracking mount located on the roof of the Radio Astronomy Observatory. The 10,700 MHz and 2700 MHz radiometers use 4-foot and 6-foot waveguide fed, parabolic reflecting antennas, respectively. The 960 MHz uses a helix fed, 6-foot parabolic reflecting antenna, while the 328 MHz radiometer uses a pair of stacked Yagi antennas.

The receivers operating at 10,700, 2700 and 960 MHz are essentially similar switched superhetrodyne receivers. The 328 MHz receiver is a total power receiver with a band-width of 80 kHz. The IF band-width of each of the other three receivers is 8 MHz. Both signal and image channels are used

The sensitivities of the receivers for which data are being reported are approximately $6.0 \times 10^{-22} Wm^{-2}Hz^{-1}$ for the 10,700 MHz system and approximately $1.0 \times 10^{-22} Wm^{-2}Hz^{-1}$ for the 2700 MHz system, and $0.5 \times 10^{-22} Wm^{-2}Hz^{-1}$ for the 960 MHz system.

The outstanding occurrences are presented in accordance with the classification scheme on page 19 of IQSY Instruction Manual No. 2 Solar Activity as reproduced on page 21.

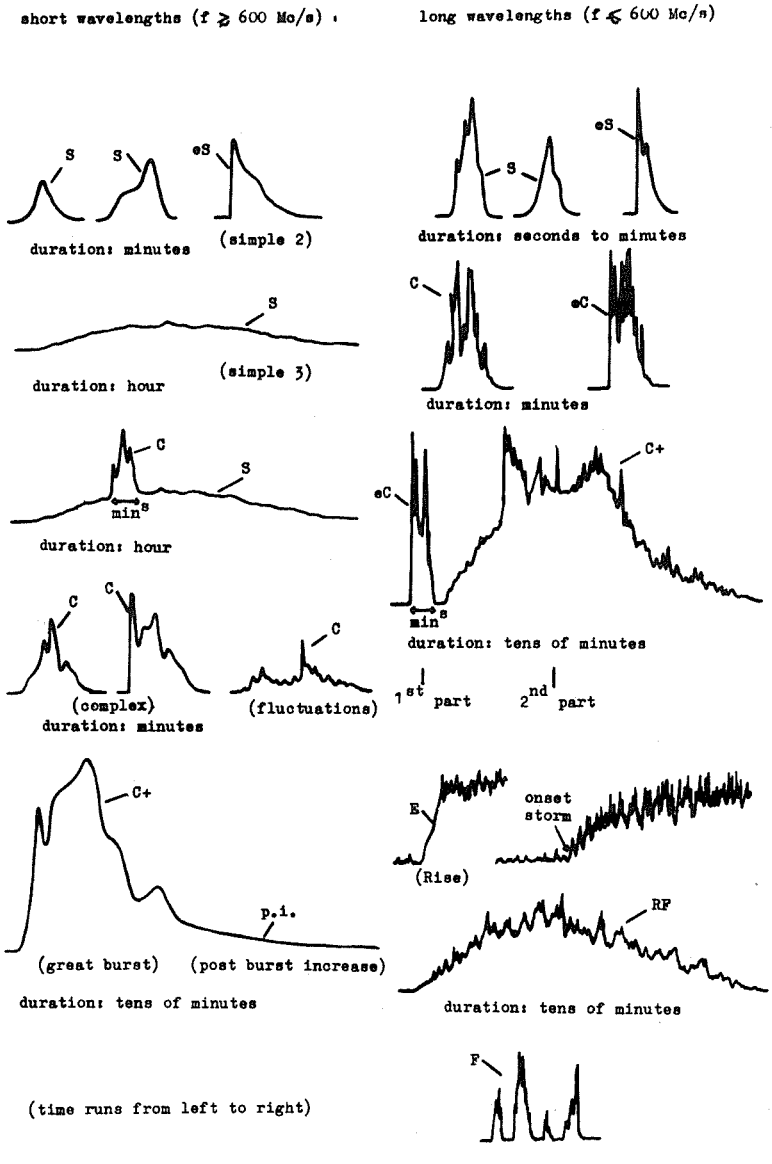

Classification of distinctive events.

15,400, 8800, 4995, 2695, 1415 and 606 MHz Sagamore Hill -- The Sagamore Hill Solar Radio Observatory of the Air Force Cambridge Research Laboratories in 1966 began operating a solar patrol of 8800, 4995, 2695, 1415 and 606 MHz. The patrol was extended to 15,400 MHz in late 1967. In 1968, coverage will be extended to the 200-300 MHz range with the installation of an additional 28 ft equatorial radio telescope. Certain portions of the project are funded by the AFCRL Laboratory Directors Fund. The objectives are to provide high absolute accuracy flux measurements at 606 and 1415 MHz (goal $\pm$ 5%) to provide coverage at other regions in the microwave spectrum with somewhat lesser absolute accuracy ($\pm$5 - 10%), and to study centimeter burst spectra for an explanation of causative mechanisms.

Solar coverage is provided from sunrise to sunset at the two longer wavelengths. A 28 foot diameter polar mounted parabola and dual frequency feed is used. At 606 MHz, the half power beam width is about 4°, while at 1415 MHz, the underilluminated parabola provides a 3° beam. The shorter wavelengths operate from a polar mounted 8 foot parabola with a multifrequency feed. Coverage is from sunrise to sunset generally, except for a period when some afternoon data will be lost due to partial antenna blockage.

The parabola is underilluminated at 8800 MHz. The 15,400 MHz system employs a 3 ft diameter parabola on a separate mount. Corrections are employed to convert apparent fluxes to true fluxes where required. Principal flux calibrations are made at about 1700 UT (meridian transit) each day; though morning and afternoon calibrations are also made.

All receivers are essentially "Dicke" radiometers. I.F. bandwidth of each is about 8 MHz, except for 606 MHz which was reduced to 2 MHz because of T.V. interference. The operating frequency of this system was also raised several megaHertz above the nominal 606 in September 1966 because of T.V. problems. Band pass filters (RF) and single side band operations are employed at 606 and 1415 MHz. The remaining receivers operate dual side band where the L.O. is designated the operating frequency. All systems employ a 30 MHz I.F.

All flux data variation resulting from the varying distance between the sun and the earth is corrected to 1 A.U. Corrections are also made for average vertical attenuations given on page 9. Outstanding occurrences are listed according to the I.A.U. classifications (See Ottawa 2800 MHz and Pennsylvania State University Diagrams).

486 MHz Washington State University -- The Washington State University radio telescope is located near Pullman, Washington, at 46°25'30"N, 117°12'W. Since January 1966, it has been operating continuously at a frequency of 486 MHz.

The antenna is a 15-foot parabolic dish with a dipole disk feed. The feed is an asymmetric dipole with a disk reflector and a matching network so that the system appears as a balanced, linear dipole to the 50-ohm transmission line. The measured antenna half-power beamwidth is 7.25°. The antenna mount and tracking system is capable of both elevation and azimuth variation. An analog computer positions the antenna on the sun. Although the antenna mount system will track in winds up to 25 miles per hour, gusts may temporarily swing the antenna away from the sun, resulting in reduced recorded noise power.

The receiver is a Dicke-type, switched, comparison, double conversion, superheterodyne system with standardized gain. The RF comparison is by a single-pole, double-throw, solid-state switch driven at 805 Hz. The comparison noise source is a 50-ohm resistor in an environmentally controlled box. The comparison noise temperature is thus the ambient temperature of the insulated box which could vary daily up to 15°K, introducing a possible error of 2% at the quiet sun level. The box, which also contains the RF amplifier, first mixer, and first IF, is mounted on the back side of the parabolic reflector. A control building, 15 feet from the mount, contains the second mixer, second IF amplifier, detectors, and recorder. To improve long-term gain stability, the system has an automatic gain control loop keyed to the standard noise source for comparison. The ambient temperature variations of the standard can produce gain changes of a maximum of 2%. The antenna signal is synchronously detected at the switching frequency, 805 Hz. The integration time is 2 seconds.

The calibration of the system is accomplished by inserting a known noise power across 50 ohms into the receiver at the antenna terminals of the RF switch and marking on the chart recorder. The calibration source is a commercial noise generator PRD-904 with a stated accuracy of 2%. Currently, the chart calibration is 130 x 10^{-22}Wm^{-2}Hz^{-1} per inch. The outstanding events are classified in accordance with the Covington scheme. Between October 1966 and May 1967, the IAU classification system was used.

A measure of the quality of this type of system is the minimum detectable change in temperature (ΔT) at the antenna terminals. Fluctuations in the record, for this system, due to gain variations are negligible when the output noise power of the comparison noise source is nearly equal to the noise power from the antenna. The ΔT, when the above applies, for this system is about 0.5°K [0.015 x 10^{-22}Wm^{-2}Hz^{-1}]. The comparison noise source of this system is a fixed source, and the ΔT will depend upon the strength of the radio source. When "looking" at the quiet sun, the ΔT is approximately 7°K [0.21 x 10^{-22}Wm^{-2}Hz^{-1}].

The characteristics of the system are tabulated as follows:

	RF Amplifier	1st IF Amplifier	2nd IF Amplifier
Center frequency	486 MHz	52 MHz	16 MHz
Bandwidth	2.8 MHz	5 MHz	2.8 MHz
Gain	33 db	60 db	40 db

System noise temperature is about 555°K [16.6 x 10^{-22}Wm^{-2}Hz^{-1}].
System noise figure is about 4.7 db.
Minimum detectable change in temperature is about 0.5°K [0.015 x 10^{-22}Wm^{-2}Hz^{-1}].
System gain is stabilized to the standard noise source.
Total expected error (largely due to uncertainty about antenna effective aperture) is about 15%.

408 MHz Observatorio de Fisica Cosmica, San Miguel, Argentina -- The Observatorio de Fisica Cosmica of San Miguel (34°28'S, 58°44'W) in late 1966 began a regular solar event patrol on 408 MHz. The geographic position of the site is advantageous in comparison with the northern hemisphere for greater time coverage of the sun in the western hemisphere.

The radiometer used is a "full power" type with antenna switching that operates only once every five minutes (both for timing and calibration) when a 50 ohm load at room temperature is substituted for the antenna at the input. Twice a day a diode noise generator is connected to calibrate the instrument. The antenna is a 5.1 meter diameter paraboloid on an equatorial mount that follows the sun from sunrise to sunset. The receiver is single sideband. Following a single stage of R.F amplification the crystal mixer feeds a cascade preamplifier tuned to 30 MHz with an overall bandwidth of 1.8 MHz. The main I.F. amplifier preceded by a step attenuator has a bias source at its second detector to set the zero of the potentiometer recorder. The total time constant is of 1.5 seconds.

The records obtained are used to calculate the daily average flux level as well as the amplitude of the bursts recorded. The antenna s.p.d.t. switch crosstalk factor is sometimes used as a means of measuring very large amplitude events at five minute intervals when the 50 ohm load is connected.

184 MHz ESSA Boulder -- Data on solar radio emission at the nominal frequency of 184 MHz recorded at the Table Mountain (Boulder) station of the ESSA Research Laboratories of the Environmental Science Services Administration are presented. The antenna is equatorially mounted and linearily polarized.

Only the outstanding occurrences are reported. Starting and maximum times in UT are read to the nearest 1/10 minute if they are very definite and otherwise to the nearest minute. The following qualifying symbols are used following the time or duration entries:

E = Event in progress before observations began.
D = Event continues after observations cease.
S = Measurement may be influenced by interference or atmospherics.

The types of the outstanding occurrences follow the classification originally described for 200 MHz observations by Dodson, Hedeman and Owren (Ap. J. 118, 169, 1953). The types are identified by numbers which describe the character of the trace, but not the magnitude of the event, as follows:

0 - Rise in base level -- A temporary increase in the continuum with duration of the order of tens of minutes to an hour.

1 - Series of bursts -- Burst or groups of bursts, occurring intermittently over an interval of time of the order of minutes or hours. Such series of bursts are assigned as distinctive events only when they occur on a smooth record or show as a distinct change in the activity.

2 - Groups of bursts -- A cluster of bursts occurring in an interval of time of the order of minutes.

3 - Minor burst -- A burst of moderate or small amplitude, and duration of the order of one or two minutes.

4 - Minor burst and second part -- A double rise in flux in which the early rise is a minor burst.

6 - Noise storm -- A temporary increase in radiation characterized by numerous closely spaced bursts, by an increase in the continuum, or by both. Duration is of the order of hours or days.

7 - Noise storm begins -- The onset of a noise storm occurs at some time during the observing period.

8 - Major burst -- An outburst, or other burst of large amplitude and more than average duration. A major burst is usually complex, with a duration of the order of one to ten minutes.

9A, 9B or 9 - Major burst and second part or large event without distinct first and second parts -- If there is a double rise in flux, the first part, a major burst, is listed as 9A and the second part as 9B. The second part may consist of a rise in base level, a group or series of bursts, a noise storm. A major increase in flux with duration greater than ten minutes but without distinct first and second parts, is listed simply as 9.

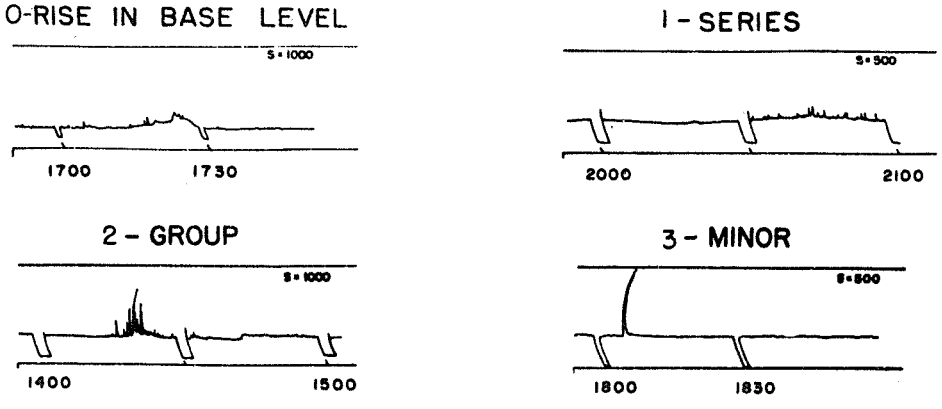

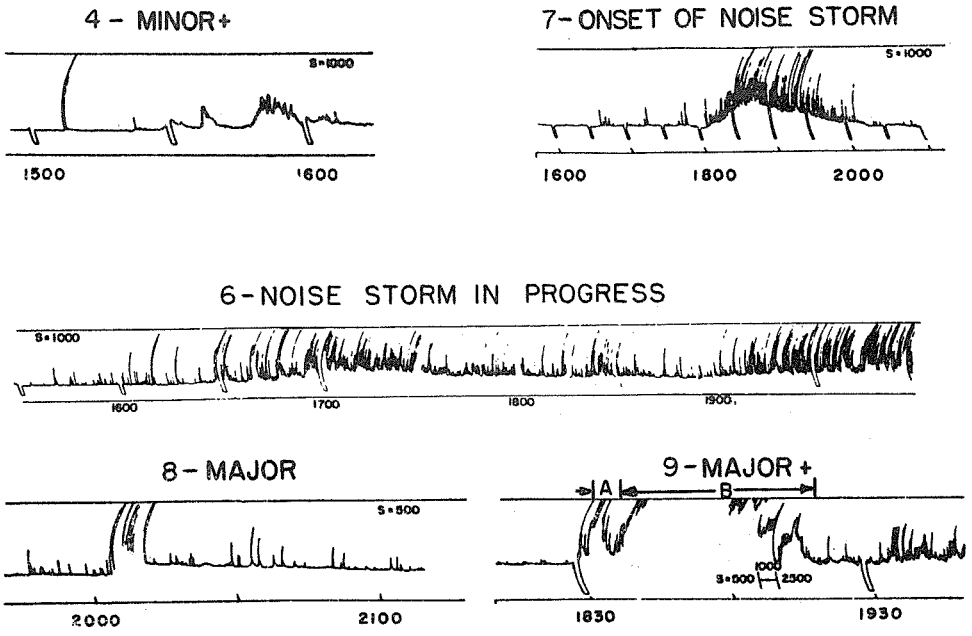

107 MHz Haleakala -- Outstanding occurrences of solar radio emission are presented at the nominal frequency of 107 MHz as recorded by the Hawaii Institute of Geophysics of the University of Hawaii at the Haleakala Observatory on Maui under the direction of Dr. John T. Jefferies. The antenna is equatorially mounted and linearily polarized. The plane of polarization is parallel to the solar rotation axis. The outstanding occurrences are reported in the same manner as for 184 MHz described above.

18 MHz McMath-Hulbert Observatory, Boulder and Haleakala -- Solar noise bursts at 18 MHz as identified on SCNA records are included whenever these reports are received in time. Prior to December 1966 these 18 MHz bursts were listed in the table for Ionospheric Effects of Solar Flares. The stations capable of making such reports are McMath-Hulbert Observatory, Pontiac, Michigan, University of Colorado, Boulder, Colorado, and Hawaii Institute of Geophysics, Haleakala.

Interferometric Observations -- Two charts present solar interferometric observations as recorded around local noon at Nançay, France (47°23'N, $8^{m}47$°E) the field station of the Meudon Observatory. For 408 MHz the plane lobes are parallel to the meridian plane: the half-power width is 1.7 minutes of arc in the East-West direction. The main lobes are about 25' apart (B. Clavelier, Comptes Rendus Acad. Science, Paris).

The records give the position and the intensity of centers observed at this frequency. These daily data are plotted on the same chart. The intensity is given in $10^{-22}Wm^{-2}Hz^{-1}$ and clearly indicated for the centers whose flux density is more than $0.20 \times 10^{-22}Wm^{-2}Hz^{-1}$. The distance between the main lobes being smaller than the radioelectrical diameter of the sun, there is sometimes an ambiguity about the position East or West of the center of activity. In this case, the two possible positions are indicated on the chart by a circle.

For 169 MHz the main lobes are parallel to the meridian plane: the half-power width is 3.8 minutes of arc in the East-West direction. The main lobes are about 1° apart (Ann. Astroph. 20, 155, 1957). The records give the strip intensity distribution from the center of the disk to 30' to the West and East.

These daily distributions are plotted on the same chart giving diagrams of evolution. Points of equal intensity given in relative units are joined day after day in the form of isophotes. Four equal intensity levels have been chosen to draw the isophotes. These intensities are proportional to 0.6, 1, 1.5 and 2. The first level corresponds to the sun without any radio storm center.

In each noisy radio region the smoothed intensity around noon is given in $10^{-22}Wm^{-2}Hz^{-1}$.

East-West Solar Scans -- Two charts present for each day an East-West strip scan of the sun, one at 21 cm and the other at 43 cm. These data are made possible by the "Fleurs" Radio Astronomy Station of the University of Sydney, Sydney, Australia. An ESSA contract provides some of the support for this work.

For the East-West solar scans from the 21 cm solar radio array the fan-beam has 2' of arc resolution. The two short horizontal lines drawn crossing the center line indicate the cold-sky level and the estimated quiet-sun level. The gain may differ from day to day. The curves have not been normalized to account for these gain variations other than the indication of the estimated quiet-sun level.

East-West solar scans are also available from a 45 cm-λ solar radio array. The fan beam has a resolution of 4' of arc. The estimated quiet sun is indicated on the published profiles in the same manner as for the 21 cm-λ scans. The curves have not been normalized for variations in gain.

SOLAR WIND VELOCITY
PIONEERS 6 AND 7

The NASA Ames Research Center plasma probe solar wind velocity data from Pioneers 6 and 7 are now being supplied by John H. Wolfe. These data include the date and time of observation in UT, the satellite pass number, the solar wind bulk velocity in kilometers per second and the co-rotation delay time in days.

The letter preceding the time of observation denotes the tracking station from which the data were acquired. "J" denotes the 85 foot antenna station at Johannesburg, South Africa and "G" denotes the 85 or 210 foot antenna at Goldstone, California.

The pass number refers to the total number of times since launch that the spacecraft has passed over the tracking station at the particular time of observation.

The solar wind velocity, U_{H+}, is derived by a computer fit of the solar wind proton energy distribution to a Maxwell-Boltzmann distribution in a moving frame of reference. The speed is given in kilometers per second and represents the bulk or convective speed of the solar wind.

The co-rotation delay, TAU, is defined as the time in days required for a steady state solar co-rotating plasma beam to rotate from the spacecraft to earth. A diagram showing the angular positions of Pioneers 6 and 7 with respect to the earth follows. As can be seen from the diagram, Pioneer 7 is lagging the earth and therefore TAU is positive whereas Pioneer 6 is leading the earth and therefore TAU is negative. The co-rotation delay depends on the heliocentric radial distance of the earth and the spacecraft, the angular separation between the earth and the spacecraft, the solar angular velocity and the solar wind bulk speed which defines the degree of the hose angle of the co-rotating interplanetary magnetic field. The equation used to compute the co-rotation delay is as follows:

$$\text{Co-rotation delay (secs)} = \text{TAU} = \frac{\phi}{W} - \frac{1}{U_{H+}}(r_p - r_e)$$

where W = 27 day solar rotation period angular velocity (in radians sec^{-1})

$= 2.6934 \times 10^{-6}$ radians sec^{-1}

ϕ = Ecliptic projection of Earth-Sun-Pioneer angle (in radians)

r_p = Ecliptic projection of Sun-Pioneer distance (in km)

r_e = Sun-Earth distance (in km)

U_{H+} = Solar wind velocity (in km sec^{-1})

ESP = Earth-Sun-Probe angle

The degree of out-of-the-ecliptic of each spacecraft is insignificant and hence is ignored in the above calculation.

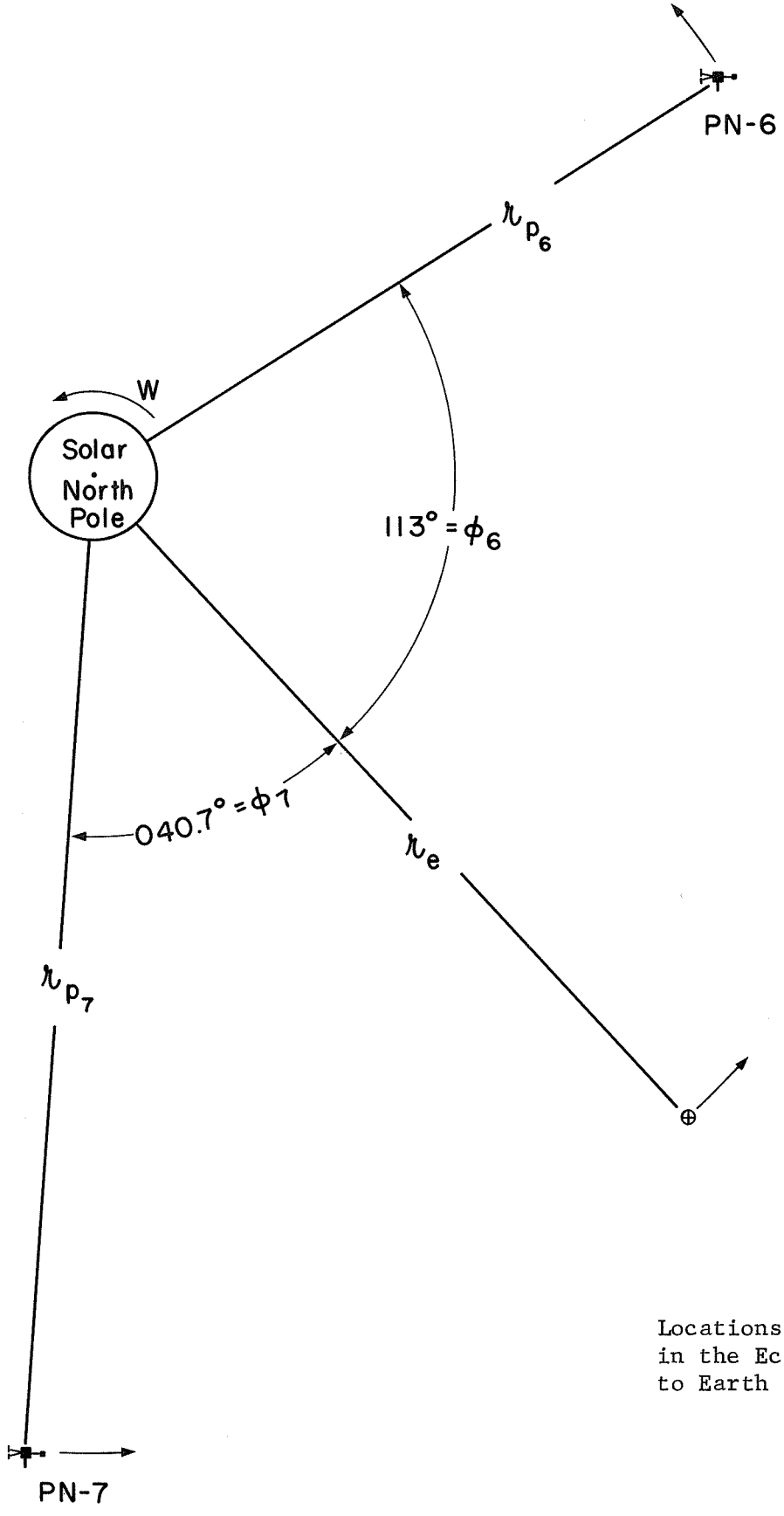

Locations of Pioneers 6 and 7 in the Ecliptic Plane relative to Earth on December 6, 1967.

SOLAR PROTON EVENTS

An unnumbered page with a diagonal slash across it will be included whenever provisional outstanding solar proton events have been reported during the month before month of publication. This will be prepared by the Space Disturbance Forecast Center of the Space Disturbances Laboratory. These sheets will be self-explanatory and are not to be used for research reference purposes, but are to be discarded when definitive data are published. They will merely provide some of the immediately available evidence when significant solar proton events have occurred in the previous month.

DATA FOR TWO MONTHS BEFORE MONTH OF PUBLICATION
TABLE OF CONTENTS

SOLAR ACTIVITY CENTERS

On one page per day are presented several photographs or charts of active solar centers recorded at optical and radio wavelengths. For each day the Carrington longitude, Lo, at 0000 UT, position angle, P, and center of sun, Bo, are given. All but one of the diagrams are reduced to the scale of the transparent Stonyhurst disks provided with this text. Though a magnifying glass is needed to read detail, it is felt that the significant regions stand out on the scale used. For those interested, copies with the solar disk at approximately 15 cm in diameter can be made available at cost through the World Data Center A Upper Atmosphere Geophysics.

These data are H-α photographs provided by the Space Disturbances Laboratory, ESSA, at Boulder, Colorado and the USAF Sacramento Peak Observatory at Sunspot, New Mexico; sunspot drawings by the Space Disturbances Laboratory, ESSA, at Boulder, Colorado; 9.1 cm and 21 cm spectroheliograms from Stanford University and Fleurs Radio Astronomy Station of the University of Sydney, respectively; a tracing of the calcium plage regions available through the McMath-Hulbert Observatory of the University of Michigan -- these are identified by the last two digits of the serial number of the plage with area in hundreds of millionths of the solar hemisphere and intensity on a scale of 1 to 5 given in a table adjacent to the tracing, (only those of intensity $\geq$ 2.5 or area $\geq$ 30 are listed); and the solar magnetogram as observed at Mount Wilson Observatory.

Details of these individual observations follow.

H-α Spectroheliograms -- These H-α spectroheliograms are furnished by the solar patrol observatory in Boulder operated cooperatively by NASA and the Space Disturbance Forecast Center of ESSA. The flare patrol instrument is a 4 1/2 inch refractor with a half-angstrom Halle filter and effective focal length of 63 inches. Typical exposure times are one-tenth second. These photographs are supplemented by observations with a similar instrument at the Sacramento Peak Observatory of the U.S. Air Force Cambridge Research Laboratories.

Sunspot Drawings -- The sunspot drawings are furnished by the solar patrol observatory of the ESSA Space Disturbance Forecast Center in Boulder under the direction of P. S. McIntosh. A 4-inch refractor is used to make drawings of 20 cm original diameter. Sunspot groups are boxed according to a judgment of bipolar pairs based on spot group evolution and the structure of associated H-α plages. Days of no observations at Boulder are usually supplemented by drawings furnished by the Sacramento Peak Observatory.

9.1 cm Spectroheliograms -- Microwave spectroheliograms are made daily at the Radio Astronomy Institute, Stanford University, Stanford, California (37°23.9'N, 122°11.3'W) under the direction of Professor R. N. Bracewell. This program is supported by ESSA.

These spectroheliograms show the distribution of microwave emission over the sun's disk as observed with a pencil beam whose East-West width to half power is 3.1', and whose North-South width varies from 3.1' in summer to nearly 6' in mid-winter (actual value 3.1' sec $(38.2° - \delta_\odot)$ at a declination $\delta_\odot$ on the meridian). For a full description of the instrument and its response see "The Stanford Microwave Spectroheliograph Antenna, a Microsteradian Pencil Beam Interferometer", IRE Transactions on Antennas and Propagation, vol. AP-9, pp. 22-30, 1961, by R. N. Bracewell and G. Swarup.

Since 1 January 1964 the maps have had 21 rows, each containing 25 temperature readings. The original maps, prior to reproduction, have 10 characters per inch horizontally and 3 lines per inch vertically, as on a typewriter; the radius of the solar disk agrees with the international standard of 7.5 cm (2.95 inches). Two + signs at the bottom of the map are 15 cm apart on the original. The center of the map, as fixed by absolute timing, is in the eleventh row, between the units and tens digits of the thirteenth reading.

Each reading of microwave emission occupies three spaces, and refers to a point on the sun centrally between the units and tens digits. The horizontal spacing of adjacent readings is about 1.63', and the vertical spacing is about 1.81'. Since the angular diameter of the sun varies with the season by about 1.7 percent, more precise values are 0.3R/2.95 and 1/3 R/2.95, where R is the sun's semi-diameter in minutes of arc taken from The American Ephemeris and Nautical Almanac. Each reading thus refers to a solid angle of about 1.63 x 1.81 square minutes of arc, or 2.50×10^{-7} steradians. We attempt to time our readings to better than 2^s absolute accuracy, or within about 0.5' at the worst in the horizontal direction. The precision with which the rows of the map are positioned on the sun's disk is a certain fraction of the North-South beamwidth, ranging from about 0.5' in summer to 1.0' in winter.

The reading printed on the map in the ith column and jth row is y_{ij} and the corresponding brightness temperature in degrees Kelvin, to the resolution allowed by the instrument, is Cy_{ij}. The unit C is currently 5000°K. (Before 1 July 1965, the unit C varied from day to day around a value of 2000°K which was stated on the map.) The readings are normalized so that the flux density S of the whole sun is equal to the absolute measurement obtained the same day on 10.7 cm by A. E. Covington at the National Research Council, Ottawa. No adjustment is made for the difference in wavelength. The formula used is

$$S = \frac{2k}{\lambda^2} C \sum y_{ij} \; (2.50 \times 10^{-7}) \left(\frac{R}{16.02}\right)^2$$

$$= 8.31 \times 10^{-28} \; C \sum y_{ij} \left(\frac{R}{16.02}\right)^2 \text{ watts m}^{-2}\text{(c/s)}^{-1},$$

where S is the flux density of the whole sun, k is Boltzmann's constant (1.38×10^{-23} joules per degree K), λ (= 9.107 cm) is the operating wavelength, and R/16.02 is the ratio of the sun's semi-diameter in minutes of arc to its mean. Active regions are emphasized by simplified contours; intended as a visual aid to interpretation, the contours refer to the 50,000 and 100,000°K levels on a smoothed map in which each reading is replaced by the mean of the nine values centered on it. Negative readings which occur do so because of the sharp cutoff in the sensitivity of the instrument to the spatial Fourier components of the source. The two-dimensional response pattern of the instrument to a point source is

$$\text{sinc } \frac{16dx}{\lambda} \text{ sinc } \frac{16d \cos (38.2^\circ - \delta_\odot)y}{\lambda},$$

where sinc $x = (\sin \pi x)/\pi x$.

Standardized spectroheliograms are available at Stanford Radio Astronomy Institute in the form of punched cards and machine-made contour charts.

Flux densities of active regions may be calculated as follows. A point source on the sun produces a peak excess brightness temperature T_p (relative to the background temperature of the adjacent quiet areas) from which the flux density S_1 of the source can be calculated using the expression

$$S_1 = \frac{2kT_p}{\lambda^2} \Omega,$$

where Ω is the effective solid angle of the antenna beam.

Now $\Omega = (\lambda/16d)^2 \sec (38.2^\circ - \delta_\odot)$, where d (= 25.00 feet) is the antenna spacing. Hence

$$S_1 = \frac{kT_p \sec (38.2^\circ - \delta_\odot)}{128d^2}$$

$$= 1.85 \times 10^{-27} T_p \sec (38.2^\circ - \delta_\odot).$$

Note: For the present the maps have not been through the computer program; therefore, please notice that the brightness value varies. In order to conform with the orientation of the other charts on the page, the map has been printed upside down, and the active centers are indicated by underlines instead of contours.

21 cm Spectroheliograms -- A daily series of radio spectroheliograms, beginning with December 1964, are presented from the "Fleurs" Radio Astronomy Field Station of the University of Sydney, Sydney, Australia, under the direction of Professor W. N. Christiansen. East-West and North-South arrays in the form of a cross give pencil beam scans with a resolution of about three minutes of arc. This program is supported by ESSA contract.

The maps show the distribution of radio emission across the solar disk at a wavelength of 21 cm by means of brightness temperature values. The unit of brightness temperature is 1700°K. It gives about the same central temperature for the quiet sun as was found at the last minimum epoch (47,000°K). The noise level is about 5 units. Contours have been sketched at levels of 50 and 100 and every 100 thereafter to draw attention to the brighter plage regions. (The level 50 Contour is shown as a broken line.) Since there is equatorial limb brightening of the quiet sun, weak radio plages in the center of the disk are discriminated against. Below each number is a dot marking the point on the disk to which the number specifically refers.

Magnetograms -- The Mount Wilson Observatory solar magnetograms are computer-plotter isogauss drawings. The polarities are indicated. "Plus" signifies the magnetic vector pointed toward the observer. The gauss levels are indicated. At times it is necessary to omit certain levels from a map because of the limited capacity of the computer. In such a case this fact is noted below the title material of each printed disk.

The observations are made with the magnetograph at the 150-foot tower telescope on Mount Wilson. The program is supported in part by the Office of Naval Research. This instrument measures the longitudinal component of the magnetic field using the line λ5250.216 Fe I. A solar magnetograph is basically a flux measuring instrument. It measures the total flux over the aperture which is being used. The magnetograph apertures are square (an image slicer is used) and the raster scan lines are separated by the dimension of the aperture. This separation of the scan lines is given by the ΔY (DELTAY) printed on the magnetogram. The units of ΔY are the units of the position orientation of the scanning system which correspond to about 0.28 arc seconds. The DELTAX represents in the same units the distance along the scan line between points at which the data were digitized.

The scan is a boustrophedonic raster scan which extends for all scan lines beyond the disk. The data within about 12 arc seconds of the solar limb are not plotted. The scanning system is always oriented so that the scan lines are perpendicular to the central meridian of the sun. The cardinal points on the magnetogram refer to heliocentric coordinates so that the "N" and "S" define the rotation axis of the sun.

The contour lines are generated by connecting straight lines between points on the scan lines representing the various gauss levels. This makes the contour map look somewhat artificial, but it emphasizes the angular resolution. Frequently there are cases where the contour line is formed from only two points - both on the same scan line. In these cases two additional points are added artificially. These points are located midway between the two real points in the scanning direction and half way to each adjacent scan line. Such contours, then, are small diamond-shaped features.

Because the magnetic field strength measured by the magnetograph is the product of the true field strength and the brightness of the image, the fields used to map the contours have been corrected for the brightness at each point. So effects of limb darkening and variable sky transparency have been corrected.

A number of errors can still be present. One of the most common of these is the zero setting of the magnetograph. At times there may be an obvious bias of the fields over the whole disk toward one or the other polarity. This will tend to show very weak features of one polarity more readily than those of the other polarity. The noise in the magnetic signal varies from day to day, but it is almost always present at the 3-gauss level. Occasionally for one reason or another a scan line may be skipped. In this case the isogauss lines will be drawn across the skipped line as if there were no scan line there. Other problems may arise from time to time. In general any feature which is present on only one day should be discounted as an artifact unless there is some particular reason to accept its reality.

Because of the difficulties with the zero offset from day to day, the polar fields will appear to vary. The polar fields can only be studied by comparing them with other weak-field regions observed on the same day.

Sometimes, because of the small scale of the reproductions, it is difficult to make out the details of the field distribution in some regions. Large scale copies of the particular magnetograms may be obtained by writing to:

World Data Center A
Upper Atmosphere Geophysics
ESSA
Boulder, Colorado U.S.A. 80302

Calcium Plage Reports -- The contours are based on estimates made and reported on the day of observation as already stated on page 8 of this text. These data on calcium plage regions are as reported by the McMath-Hulbert Observatory of the University of Michigan supported by ESSA contract. They are the same regions which have been summarized in the table described on page 10. Listed beside the drawings in each case are the plages with intensity ≥ 2.5 or size ≥ 3000 millionths of the solar hemisphere.

CORONAL LINE EMISSION INDICES

Emission intensity indices for each quadrant of the limit for the λ5303 (FeXIV) and λ6374 (FeX) coronal lines are listed in the table. The indices are based on measurements made at 5° intervals around the periphery of the solar disk by Pic-du-Midi and Kislovodsk. Measurements by the High Altitude Observatory at Climax, Colorado and the USAF Sacramento Peak Observatory at Sunspot, New Mexico will be included as soon as they again become available. The measurements are expressed in millionths of an angstrom of the continuum of the center of the solar disk (at the same wavelength as the line) that would contain the same energy as the observed coronal line. The indices are:

G_6 = mean of six highest line intensities in quadrant for λ5303.

G_1 = highest value of line intensity in quadrant for λ5303.

R_6 = mean of six highest line intensities in quadrant for λ6374.

R_1 = highest value of line intensity in quadrant for λ6374.

The dates given in the table correspond to the approximate time of CMP of the longitude zone represented by the indices. The actual observations were made for the northeast and southeast quadrants 7 days before; for the southwest and northwest quadrants 7 days after the CMP date given.

To obtain rough measures of the integrated emission of the entire solar disk in either of the lines, assuming the coronal changes to be small in a half solar rotation, it is satisfactory to perform the following type of summation given in example for 15 October:

$$\left(\begin{matrix}\text{MEAN DISK EMISSION}\\ \text{IN } \lambda 5303\end{matrix}\right)_{15\ \text{OCT}} = \frac{1}{N}\left[\sum_{15\ \text{OCT}}^{22\ \text{OCT}}\left\{(G_6)_{NE}+(G_6)_{SE}\right\}+\sum_{8\ \text{OCT}}^{14\ \text{OCT}}\left\{(G_6)_{SW}+(G_6)_{NW}\right\}\right]$$

where N is the number of indices entering the summation.

Such integrated disk indices as well as integrated whole-sun indices can be computed for each day. For past years they were published by the High Altitude Observatory at Boulder, Colorado.

SUDDEN IONOSPHERIC DISTURBANCES

SID, sudden ionospheric disturbances (and GID, gradual ionospheric disturbances) may be detected in a number of ways: shortwave fadeouts (SWF), increases in cosmic absorption (SCNA), enhancement of low frequency atmospherics (SEA), sudden phase anomalies at VLF (SPA), sudden enhancements at VLF (SES) and sudden frequency deviations (SFD).

The table on page 39 of this text gives the two-letter station code used in the published data table. The geographic location of the station and the type or types of SID information submitted are indicated. These data are made possible through the auspices of the International Ursigram and World Days Service, the Smithsonian Astrophysical Institute, and the U.S. Coast Guard. Greater detail concerning the reporting stations can be found in "The Listing of Sudden Ionospheric Disturbances" by J. Virginia Lincoln (Planet. Space Sci. 12, 419-434, 1964) and in earlier versions of this text.

SWF -- SWF events are recognized on field-strength recordings of distant high-frequency radio transmissions.

In the coordinated program, the abnormal fades of field strength not obviously ascribable to other causes, are described as shortwave fadeouts with the following further classification:

S-SWF (S) : sudden drop-out and gradual recovery
Slow S-SWF (SL): drop-out taking 5 to 15 minutes and gradual recovery
G-SWF (G) : gradual disturbance: fade irregular in either drop-out or recovery or both.

When there is agreement among the various reporting stations on the time (UT) of an event, it is accepted as a widespread phenomenon and listed in the table.

The degree of confidence in identifying the event, a subjective estimate, is reported by the stations and this is summarized in an index of certainty that the event is geographically widespread, ranging from 1 (possible - single station) to 5 (definite - many stations). The times given in the table for the event are from the report of a station (listed first in the group of stations) that identified it with high confidence. The criteria for the subjective importance rating assigned by such station on a scale of 1- to 3+ include amplitude of the fade, duration of event and confidence of reality of event. The published summary importance rating is also subjective with greater consideration given to reports on paths near the subsolar point for the particular event.

SCNA-SEA -- Sudden ionospheric disturbances next listed in the table are those which have been recognized on recorders for detecting cosmic absorption at about 18 MHz (SCNA) or on recorders for detecting enhancements of low frequency atmospherics at about 27 kHz (SEA).

STATION LIST FOR SUDDEN IONOSPHERIC DISTURBANCES TABLE

CODE	STATION LOCATION	SWF	SCNA	SEA	SES	SFD	SPA
AN	= ANCHORAGE, ALASKA	X	X				X
AT	= ATHENS, GREECE	X					
BA	= BARBADOES, B.W.I.	X					
BE	= FT. BELVOIR, VIRGINIA	X					
BN	= BRENTWOOD, ENGLAND	X					
BO	= BOULDER, COLORADO	X	X	X		X	X
BY	= BEARLEY, ENGLAND	X					
CA	= CANBERRA, AUSTRALIA	X	X				
CR	= CARNARVON, AUSTRALIA	X					
DA	= DARMSTADT, GFR	X					
DE	= DEBRE ZEIT, ETHIOPIA						X
*DV	= PATERSON, NEW JERSEY				X		
GH	= GODLEY HEAD, N.Z.	X					
GS	= GREENBELT, MARYLAND	X					
HA	= MAUI, HAWAII		X	X		X	X
HK	= HONG KONG, B.C.C.	X					
HU	= HUANCAYO, PERU	X					
JU	= JUHLESRUH, GDR	X	X	X			
KE	= KERGUELEN ISLAND		X	X			X
KU	= KUHLUNGSBORN, GDR	X	X	X			X
LO	= PRESTON, ENGLAND			X			
MA	= MANILA, PHILIPPINE ISLANDS	X	X	X			X
MC	= PONTIAC, MICHIGAN	X	X	X			
ND	= NEW DELHI, INDIA	X	X	X	X	X	X
OK	= OKINAWA, PHILIPPINES	X					
PO	= POITIERS, FRANCE	X		X			
PU	= PRAGUE, CZECHOSLOVAKIA	X	X	X			X
RO	= ROME, ITALY		X	X			
SL	= SLOUGH, ENGLAND						X
SN	= SAN FERNANDO, SPAIN						X
SO	= SOMERTON, ENGLAND	X					
SW	= ENKOPING, SWEDEN	X					
SY	= SYDNEY (CULGOORA), AUSTRALIA	X					
TA	= HOBART, TASMANIA			X			
TK	= TOKYO, JAPAN						X
TO	= HIRAISO, JAPAN	X					
TR	= ST. AUGUSTINE, TRINIDAD, B.W.I.	X					
TS	= TORTOSA, SPAIN			X			
TY	= TOYOKAWA, JAPAN			X			
UM	= SAO PAULO, BRAZIL				X		X
WO	= WOOMERA, AUSTRALIA						X
WS	= WHITE SANDS, NEW MEXICO	X					

AMERICAN ASSOCIATION OF VARIABLE STAR OBSERVERS

A1	= VALLEY COTTAGE, N.Y.			X	X		
A2	= PITTSBURG, PA.			X			
A6	= OSHKOSH, WIS.			X			
A8	= HADDAM, CONN.			X			
A17	= DURBAN, SOUTH AFRICA			X			
A18	= SCITUATE, MASS.			X	X		
A19	= LATROBE, PA.			X			
A20	= WEST NYACK, N.Y.				X		
A21	= LITTLETON, COLO.			X			

LORAN-C SKYWAVE MONITOR STATIONS

CP	= CAPE RACE, NEWFOUNDLAND				X		X
GE	= GESASHI, OKINAWA				X		X
HO	= HOKKAIDO, JAPAN				X		X
JP	= JUPITER, FLORIDA				X		X
KR	= KURE				X		X
MR	= MARCUS				X		X
NT	= NANTUCKET ISLAND, MASSACHUSETTS				X		X
PC	= PORT CLARENCE, ALASKA (NOME)				X		X
SA	= SANDUR, ICELAND				X		X
SK	= SITKINAK, ALASKA				X		X
ST	= SYLT, GERMANY				X		X
TT	= ATTU, ALEUTIAN ISLANDS				X		X
UP	= UPOLO POINT, HAWAII				X		X
YP	= YAP				X		X

* DV is former AAVSO member designated as A3.

These reports are coordinated at ESSA Boulder. When there is agreement among the various reporting stations on the time (UT) of an event, it is accepted as a widespread phenomenon and listed in the table. Some phenomena are listed, if noted at only one location, if there has been a flare or another type of flare-associated effect reported for that time.

In the table under the type of event the subjective importance of the event is given on a scale of 1 minus to 3 plus. Next there is the index of geographic widespread certainty ranging from 1 (possible) to 5 (definite). The times of beginning, end and maximum phase of the event in UT are given as reported by the station listed first in the group of observing stations. If the event is an SCNA, a percent absorption figure is given. This absorption is calculated by the formula:

$$\text{SCNA } \% = \frac{I_n - I_f}{I_n} \times 100$$

where I_n = noise diode current required to give a recorder deflection equal to that which would have occurred in the absence of a flare, i.e. a value extrapolated from cosmic noise level trend before and after a flare. The previous day's record may be considered if necessary.

and I_f = noise diode current required to give a recorder deflection equal to the level at the time of maximum absorption.

SPA and SES -- Sudden phase anomalies (SPA) are observed as a phase shift of the downcoming skywave on VLF recordings or on pulse measurements on LF recordings. An estimate of the intensity can be obtained in terms of the degree of phase shift (see Chilton, C.J. et al, Jour. Geophys. Res. 68, 5421-5436, October 1, 1963). The length of path and amount of sunlight on the path must of course be considered.

In the table under SPA column for VLF recordings the degrees of phase change are given for the path reporting maximum phase change, while under the station column the parenthetical remark gives an abbreviated code of the call letters and frequency (See code list below), together with the degrees of phase change for each VLF transmitter recorded at the observing station. For each event the time of beginning, time of maximum phase advance, and time of ending in UT are given.

Sudden enhancements of signal strength (SES) are observed on field-strenth recordings of extremely stable VLF transmissions. The times of beginning, ending and maximum are given in UT, as well as a subjective importance rating from 1- to 3+ as in the column headed SES and a widespread index as described under SWF above.

Code Abbreviations

M = NPM, Honolulu, Hawaii
C = NWC, North West Cape, Australia
AA = NAA, Cutler, Maine
A = NBA, Balboa, Canal Zone
K = NLK, Jim Creek, Washington
G = NPG, Jim Creek, Washington
S = NSS, Annapolis, Maryland
R = GBR, Rugby, England
L = WWVL, Ft. Collins, Colorado
B = WWVB, Ft. Collins, Colorado
O = Omega 10.2 MHz, Haiku, Hawaii
12.0 MHz, Trinidad, B.W.I.
13.6 MHz, Aldra, Norway

Thus, for VLF frequencies the transmitter will be identified by a one or two-letter code followed by the frequency.

SPA recorded by LF pulse observations over a one hop propagation path yield information more indicative of the ionospheric changes occurring at the mid-point of the path, rather than over the entire path. LF phase observations, reported in degrees, represent an increase in sensitivity over VLF observations. The phase sensitivity is directly proportional to the ratio of the frequencies for identical paths. However, since the height of energy deposition is related to the type of flare x-rays emitted, the LF measurements in conjunction with the VLF measurements will tend to indicate the x-ray intensity range. Since the LF signal can apparently be reflected from either of two layers within the D-region (see Doherty, R.H., Radio Science, 2, 645-651, June 1967), phase retardations as well as phase advances may occur during an SID.

The amplitude of the low frequency pulse observations made at Loran stations normally changes during an SID. This change is usually, but not always, in the direction of a signal enhancement (SES). The height of signal absorption is below the height of signal reflection. LF amplitude observations along with the LF and VLF phase observations for any one event tend to indicate the x-ray intensities associated with that event. Amplitude changes are reported in db to the nearest db of voltage change. Since 6 db represents doubling of the received signal and 20 db represents a ten fold change im amplitude, it is obvious that many SIDs produce large effects in LF propagation.

Beginning soon, SPA and SES measurements will also be published from data observed by LF Loran-C stations. These stations record pulse measurements on 100 kHz. As part of the Loran-C sky-wave monitoring program, stations within each chain transmit to one another. Examples of the identification of the Loran stations whose events are presented in the SID table are as follows:

MR-HO signifies the reported data were recorded by MR monitoring HO, followed by a slash and the phase angle shift;

MR-HO-MR signifies the reported event was recorded by MR monitoring HO, and by HO monitoring MR when the SPA values were within 20° of each other or the SES values were within 3 db of each other and the stations are followed by a slash and the higher of the phase angle shifts or of the db values.

See table on page 39 for code letters and locations of Loran-C stations.

SFD -- A sudden frequency deviation (SFD) is an event where the received frequency of an HF radio wave reflected from the ionosphere increases suddenly, peaks, and then decays back to the transmitted frequency. Sometimes several peaks occur and usually the frequency deviation takes on negative values during the decaying portion of an SFD. The largest SFD observed at Boulder had a peak frequency deviation of about 61 Hz. The peak frequency deviation for most SFDs is less than 0.5 Hz. The start-to-maximum time is typically about 1 minute. SFDs are caused by sudden enhancements of ionization at E and F1 region heights produced by impulsive flare radiation at wavelengths longer than 4 Å. Flashes of radiation at wavelengths longer than 100 Å contribute to most SFDs. A more complete discussion of SFDs can be found in "An Investigation of Sudden Frequency Deviations Due to the Immediate Ionospheric Effects of Solar Flares" by R. F. Donnelly, ESSA Technical Report No. I.T.S.A. 19, January 1967.

SFDs are presently observed at Boulder (BO) on frequencies near 2.1, 3.3, 4, and 5.1 MHz with near-vertical propagation (station call letters KKE42) and on frequencies near 8.9, 9.9, 11.1, 12.1, and 13 MHz transmitted from near Havana, Illinois (WWI) to Boulder (1290 km). SFD observations at Boulder on WWV have been discontinued since WWV has moved from Virginia to Colorado. SFD observations made in New Delhi on JJY and at the University of Hawaii Dept. of Electrical Engineering on WWVH at 5, 10, and 15 MHz will be reported with the station abbreviations ND and HA respectively.

The number entered in the SFD column of the table gives the peak frequency deviation in tenths of Hz. The entry in the same row in the stations column gives the corresponding station location, transmitter call letters, and the approximate frequency in Hz. For example, a "12" in the SFD column followed by HA(WWVH5) in the stations column means the peak frequency deviation observed by the University of Hawaii on 5 MHz WWVH was 1.2 Hz.

SID Table -- To summarize the table lists these phenomena jointly giving: date, beginning, ending and maximum phase in UT; a geographically widespread index for type of event; type and importance rating if SWF; percent absorption and importance if SCNA; importance if SEA; degrees of phase change if SPA with path designated; importance if SES or db if LF path; the peak frequency deviation in tenths of Hz if SFD and stations observing event. In the tables D = greater than, E = less than, and U = approximate for times indicated.

SOLAR X-RAY RADIATION

The data published two months after observation consist of tables of observing times, solar x-ray flux daily averages, and outstanding events. Sources of the data are the Naval Research Laboratory's X-Ray Monitoring Experiments on NASA's OGO-4 and OSO-4 Satellites. The instrumentation for these experiments consists of four photometers in each satellite covering the 0.5-3, 1-8, 8-16, and 44-60 Angstrom bands. The Naval Research Laboratory's Solar X-Ray Monitoring Satellite (1965-93A) was also a data source until it ceased to transmit useful data on 7 December 1967. This program is under the direction of Robert W. Kreplin.

The column entries are explained below:

Daily Average X-ray Flux Indices -- The average x-ray flux index for each day is calculated from individual records made during the intervals listed in the table of observing times. Four x-ray bands are normally monitored but because of the great variability observed in the 0.5-3 A band these data are not included in the table of daily averages.

44-60 A Index -- The reduction of the 44-60 A photometer signal to flux values involves the use of a "gray body" approximation (Kreplin, R. W., Ann. Geophys. 17, 151-161, 1961) in which a temperature of 0.5×10^6 °K is used to define the wavelength distribution. Austin, Purcell, and Tousey (Astron. J. 69, 133, 1964) have photographed a line spectrum in the region 44-60 A. Unit quantitative measurements of the line intensities are made for this region, the 44-60 A flux levels must be used with some reservation. Comparisons of flux values at different times can, however, be made with an accuracy set by a standard deviation of about 2% in the flux value obtained from the record of an individual satellite pass during quiet solar conditions.

8-16 A Index -- The 8-16 A flux index is calculated on the assumption that this region of the solar spectrum may be approximated by a 2×10^6 °K "gray body".

Measurement of the solar spectrum between 13 and 26 Angstroms by Blake, Chubb, Friedman and Unzicker (Astrophys. J. 142, 1-12, 1965) has revealed a number of emission lines thus the same qualifications must be made in assigning error to the absolute flux values as we made in the case of the 44-60 A index.

The standard deviation in the average flux is about 8% for this band.

1-8 A Index -- The flux in this spectral range is calculated using a 2×10^6 °K "gray body" approximation. For purposes of comparison of the flux indices a standard deviation of about 15% in the average flux value computed for a single pass may be used.

0-3A Index -- The flux in the 0.5-3A spectral range is calculated using a 1×10^7 ^{o}K "gray body" approximation.

Outstanding Events -- In this table are listed those intervals and flux indices when the flux in the 1-8 A and 0-3A bands was significantly different from the average for the day or when a change in flux value with time was observed. In this table the 44-60 A index is omitted because of the relatively small changes observed with solar activity. Start is the time of commencement of the period of solar observation during which the outstanding event occurred. End is the time of termination of the period of solar observation during which the oustanding event occurred.

Comments -- Definitions of some of the more commonly used comments are:

Peak 0000 - The time at which the flux reached the listed maximum values.
Decreasing - The flux was at a high value at start, and decreasing.
Increasing - The flux was at a high value at end, and increasing.
Read 0000 - The time at which the listed flux values were observed.

Times of Observation - These are the intervals of time (UT) when data from OGO-4 and OSO-4 were available. Intervals have not been included when x-ray flux levels showed that the satellite was in darkness.

SOLAR RADIO EMISSION

SPECTRAL OBSERVATIONS

Solar spectral events from Fort Davis (Texas), Culgoora (Australia), Boulder (Colorado) and Sagamore Hill (Massachusetts) are presented in a combined table. The contents of the table are described below:

Greenwich date

Observing periods during day (UT) -- aligned with first burst from observatory

Station -- HARV = Fort Davis, CULG = Culgoora, BOUL = Boulder and SGMR = Sagamore Hill

Burst indicated in wavelength band by beginning and ending times in UT together with an indication of intensity on a 1 to 3 scale, 3 the most important

Spectral type --
- I = storm bursts
- II = slow drift bursts
- III = fast drift bursts
- IV = prolonged continuum
- V = brief continuum (normally following type III bursts)
- CONT = continuum in close association with type III burst storms, often with reverse drift bursts and often, but not always, associated with noise storms on metric wavelengths (used by BOUL and SGMR
- UNCLF = unclassified activity

See J. P. Wild, S. F. Smerd and A. A. Weiss, Annual Review of Astronomy and Astrophysics, 1, 291, 1963 for description of types I through V.

Symbols appended to spectral type

- B = Single burst
- C = Small group (<10) of bursts
- GG = Large group (>10) of bursts
- C = Underlying continnum (particularly with type I)
- S = Storm in the sense of intermittent but apparently connected activity
- N = Intermittent activity in this period
- U = U-shaped burst of Type III
- RS = Reverse slope burst
- DP = Drifting pairs
- DC = Drifting Chains
- H = Herringbone

The bursts are divided into dekameter, meter, and decimeter wavelength ranges. For the reporting stations listed below, these ranges cover the frequency bands 10-30, 30-300, and 300-600 MHz.

Harvard Radio Astronomy Station, Fort Davis, Texas -- Summaries are presented of solar radio bursts recorded in the frequency range 10-580 MHz. The research program is supported by financial assistance from the Air Force Cambridge Research Laboratories and the Sacramento Peak Observatory. The equipment used at the Station has been described earlier (Thompson, Astrophys. J. 133, 643, 1961).

At 100 MHz the intensity ranges listed as 1, 2, and 3 correspond approximately to 5-50, 50-500, and >500 x $10^{-22} Wm^{-2} Hz^{-1}$.

Culgoora Solar Observatory, Australia -- The observations at C.S.I.R.O. Solar Observatory, Culgoora, N.S.W. Australia (30°18'56"S, 149°33'40"E) are made by the C.S.I.R.O. Division of Radiophysics, Epping, N.S.W. Summaries are presented of solar radio bursts in the frequency range 10-210 MHz. The equipment used has been described by J. P. Wild, J. D. Murray and W. C. Rowe in Australian J. Phys, 7, 439, 1954 and by K. V. Sheridan, Proc. I.R.E. Australia, 24, 174, 1963. The intensity scale is qualitative.

Astrogeophysics Department, University of Colorado, Boulder, Colorado -- Data are presented on solar radio emission in the frequency range 7.6 to 41 MHz scanned in 0.65 seconds as recorded by the Astrogeophysics Department of the University of Colorado, Boulder, Colorado. The research program is supported by ESSA and the National Science Foundation.

The collecting area of the antennas is approximately 1000 square meters, in two corner reflectors forming an interferometer pair. On the low-frequency side, bursts are frequently limited by an external reflection of the waves above the ionosphere. Examples of Type III (fast drift) and continuum records taken with this equipment are published in A. Boischot, R. H. Lee, and J. W. Warwick, Ap. J. 131, 61 1960. Type II is detected not only by means of the (relatively small) enhancement it produces against a background of continuum, but also by means of the fast fluctuations of fringe position produced as the burst drifts through the low-frequency range. Continuum of two kinds is reported: (a) in close association with Type III burst storms, and often also with reverse drift bursts. This is described simply as "continuum" (cont) and is often, but not always, associated with noise storms on metric wave lengths; (b) following major outbursts of Type III or Type II associated with flares. These latter cases of continuum are labelled Type IV in the tables. Intensities are on a rough scale from 1 to 3 corresponding approximately to 5-20, 20-80, and 80-300 (or greater) x $10^{-22}Wm^{-2}Hz^{-1}$. Above about 30 x $10^{-22}Wm^{-2}Hz^{-1}$, the equipment saturates and does not indicate relative intensities satisfactorily.

Sagamore Hill Radio Observatory, Massachusetts -- Data are presented on solar radio emissions in the frequency range 19 to 41 MHz as recorded by the AFCRL Sagamore Hill Radio Observatory. This research program is sponsored by the Air Force Cambridge Research Laboratories. Geographic coordinates of the observing site are: latitude 42°37'51.2"N, longitude 70°48'55.4"W.

The spectral range is scanned once per second. Two log-periodic antennas mounted on a 270 meter East-West baseline are used in a phase-switched interferometer receiver system. Fringe patterns obtained from solar emission provide positive identification of solar events against the background interference levels. No intensity values for the events are provided.

COSMIC RAY INDICES

Tabulated Observations -- The table presents the daily (UT) average counting rates per hour (scaled) for four high counting rate neutron monitors, Churchill, Deep River, Climax and Dallas. These monitors have different values of magnetic cutoff rigidity, while their asymptotic cones of acceptance "look" approximately in the equatorial plane in essentially the same direction in space. The four sets of data can therefore be used to estimate the rigidity dependence of fluctuations which occur in the primary cosmic radiation.

The characteristics of the four stations are given below; the data have been corrected using the listed barometric coefficients to the listed mean station pressures.

Station	Churchill	Deep River	Climax	Dallas	Alert
Geog. Lat., N.	58°45'	46°36'	39°22'	32°47'	82°30'
Geog. Long., W.	94°05'	77°30'	106°11'	96°48'	62°20'
Cut Off, BV	< 0.21	1.02	3.03	3.98	0.00
Altitude, m	39	145	3400	208	sea level
Detector type	NM64	NM64	IGY	NM64	NM64
Scaling factor	120	300	*100	120	100
Baro. coeff. %/mm. Hg.	.971	.987	.943	.971	.987
Mean press., mm. Hg.	757.6	747	504	746.3	752

* from January 1, 1966

The Climax, Colorado, USA, neutron monitor, station B305, data are communicated by J. A. Simpson and G. Lentz of the Enrico Fermi Institute for Nuclear Studies, University of Chicago. The instrument is a standard Chicago type neutron monitor, utilizing 12 BF_3 counter tubes. The station has a mean barometric pressure of 504.0 mm Hg. For a more detailed description of the neutron intensity monitor and its associated electronics see J. A. Simpson "Annals of the IGY",

Vol. IV, Part VII, pp. 351-373 (1957). The publication of these data in this monthly series began September 1960. Earlier data, beginning June 1957, are available in bihourly form at the World Data Center A for Upper Atmosphere Geophysics.

The Dallas, U.S.A. and Churchill, Canada, neutron monitors follow the IQSY design described by Carmichael (IQSY INSTRUCTION MANUAL No. 7). The Dallas reference pressure was 1000 mb until 6 August 1965, being changed from that date to 995 mb. The Churchill reference pressure is 1010 mb. The attenuation length used in the pressure correction for both stations is 137.2 mb. The data have not been corrected for the minor changes (<1%) in efficiency of monitor which inevitably occur over any appreciable period of time. The Dallas monitor is operated by Drs. K. G. McCracken (on leave of absence) and R. A. R. Palmeira of the Southwest Center for Advanced studies, Dallas, Texas, while the Churchill monitor is operated by the above, in collaboration with Dr. D. C. Rose of the National Research Council of Canada. The Technical Support Section of the Churchill Research Range is responsible for the day-to-day maintenance of the Churchill monitor. The Dallas monitor commenced operation on 1 December 1963, while the Churchill monitor commenced operation on 18 April 1964. Hourly mean data from both installations are routinely distributed to the scientific community by the Cosmic Ray Laboratory, Southwest Center for Advanced Studies, P.O. Box 30365, Dallas, Texas, U.S.A., 75230.

The Deep River, Ontario, Canada, neutron monitor, station B211, follows the IQSY design (IQSY Instruction Manual No. 7). Publication of the daily rates in this series began in January 1966 but a monthly chart of hourly values from Deep River, described below, has been published herein since January 1959. The original data can be obtained from Atomic Energy of Canada Ltd., Chalk River, Ontario, Canada, or from any of the World Data Centers.

Chart -- The chart depicts the variations of cosmic ray intensity recorded by the IQSY design 48-NM-64 neutron monitor at Deep River, Ontario, Canada, as submitted by H. Carmichael and J. F. Steljes of Atomic Energy of Canada Ltd., Chalk River, Ontario. The vertical scale lines mark the days of the month in Universal Time: the horizontal scale lines are at intervals of 5% based upon 1.846×10^6 counts per hour (after barometric correction) arbitrarily taken as 100%. The charts have been published from January 1959, publication beginning in the November 1960 issue. From January 1959 to April 1962 a smaller monitor was used and the 100% counting rate was 0.0555×10^6 counts per hour. From May 1962 to January 1965 the monitor was of intermediate size and the 100% counting rate was 0.555×10^6 counts per hour. A preliminary barometric coefficient was used from May 1962 to October 1962; in the March 1963 issue final revised charts were published for these six months using a better value of the barometric coefficient.

Beginning with the chart for July 1966 the variations of cosmic ray intensity as recorded by the IQSY design 18-NM-64 neutron monitor at Alert, North West Territories, Canada, are also presented. The Alert graph is plotted on the same scale but percentages are given for Deep River only. The Alert graph is normalized so that 100% is 0.6678×10^6 counts per hour and the 100% level is normally at 110% on the Deep River scale.

The Alert station is unique because its asymptotic cone of acceptance in space is less than 10° wide and is aligned within 7° of the spin axis of the earth. Hence, unlike the other four stations whose cones of acceptance rotate with the earth approximately in the plane of the ecliptic, Alert always "looks" into a fixed cone directed northwards. It experiences negligible periodic diurnal intensity variation.

The monitor at Alert was provided and is maintained by Atomic Energy of Canada but it is housed in a building provided by the National Research Council of Canada. Day-to-day operation is by courtesy of the Canadian Meteorological Service.

GEOMAGNETIC ACTIVITY INDICES

Kp, Ci, Cp, Ap, and Selected Quiet and Disturbed Days -- The data in the table are: five quiet days (QQ), ten quiet days (QQ or Q), and five disturbed days (D) adjacent to date; three-hour range indices Kp; international character figure, Ci; character figure, Cp (standardized Ci); and daily "equivalent amplitude", Ap. As a footnote to the table preliminary storm sudden commencements are given.

The data are made available by the Permanent Service of Geomagnetic Indices of IUGG: Association of Geomagnetism and Aeronomy through Commission IV: Magnetic Activity and Disturbances. The Meteorological Office, De Bilt, Holland, collects the data from magnetic observatories distributed throughout the world, and compiles the Ci and selected days data. Göttingen University computes the planetary and equivalent amplitude indices. The same data are also published in the Journal of Geophysical Research.

Kp is the mean standardized K-index from 12 observatories between geomagnetic latitudes 47 and 63 degrees. The scale is 0 (very quiet) to 9 (extremely disturbed), expressed in third of a unit, e.g., 5- is 4 and 2/3, 5o is 5 and 0/3, and 5+ is 5 and 1/3. This planetary index is designed to measure solar particle-radiation by its magnetic effects, specifically to meet the needs of research workers in the other geophysical fields.

The Ci-figure is the arithmetic mean of the subjective classification by all observatories of each day's magnetic activity on a scale of 0 (quiet) to 2 (storm).

The Cp-figure is a standardized version of the Ci-figure and is derived from the indices Kp by converting the daily sum of ap into the range 0.0 to 2.5.

Ap is a daily index of magnetic activity on a linear scale rather than on the quasi-logarithmic scale of the K-indices. It is the average of the eight values of an intermediate 3-hourly index "ap", defined as one-half the average gamma range of the most disturbed of the three force components, in the three-hour interval at standard stations; in practice, ap is computed from the Kp for the 3-hour interval. The extreme range of the scale of Ap is 0 to 400. Values of Ap (like Kp and Cp) have been published for 1932 to 1961 in IAGA Bulletin No. 18 by J. Bartels, distributed by North-Holland Publishing Company, Amsterdam.

The magnetically quiet and disturbed days are selected in accordance with the general outline in Terr. Mag. (predecessor to J. Geophys. Res.) 48, pp. 219-227, December 1943. The method in current use calls for ranking the days of a month by their geomagnetic activity as determined from the following three criteria with equal weight: (1) the sum of the eight Kp's; (2) the sum of the squares of the eight Kp's; and (3) the greatest Kp.

Chart of Kp by Solar Rotations -- Monthly a graph of Kp is given for eight solar rotations, furnished through the courtesy of the Geophysikalisches Institut of the University of Göttingen. Annually a graph of the whole year by solar rotations is included. From time to time another 27-day rotation chart depicting the daily geomagnetic character figure, C9, is presented. C9 is obtained from Cp by reducing the Cp-values to integers between 0 and 9 according to the key given in the charts.

The activity indices are described by J. Bartels in Annals of the IGY, Vol. IV, pp. 227-236, London Pergamon Press 1957. Below the chart of Kp a table of Ap indices for the last 12 months is presented so that trends in magnetic activity can be easily followed.

GEOMAGNETIC OBSERVATORIES

Code	Station	Geomag. Latitude
AABA	Addis Ababa	5.4N
ALIB	Alibag	9.6N
AMBE	Amberley	47.7S
ANNA	Annalmalainagar	1.5N
APIA	Apia	16.1S
BANG	Bangui	4.8N
BINZ	Binza	3.4S
BOUL	Boulder	49.0N
COLL	College	64.6N
ELIZ	Elizabethville	12.7S
FRED	Fredericksburg	49.6N
GNAN	Gnangara	43.2S
GUAM	Guam	4.0N
HRMN	Hermanus	33.3S
HONO	Honolulu	21.1N
HUAN	Huancayo	0.6S
HYDE	Hyderabad	7.6N
IRKU	Irkutsk	40.8N
KGLN	Port-aux-Francais	57.3S
MBOR	M'Bour	21.3N
MIQR	Macquarie Island	61.1S
MWSN	Mawson	73.1S
PILR	Pilar	20.2S
PMOR	Port Moresby	18.6S
SJUA	San Juan	29.9N
SITK	Sitka	60.0N
TOOL	Toolangi	46.7S
TVAN	Trivandrum	1.1S
TUCS	Tucson	40.4N
WKES	Wilkes	77.7S
WITT	Witteveen	54.1N

Principal Magnetic Storms --

Finally a table presents the principal magnetic storms for the month as reported by several observatories through cooperation with the International Association of Geomagnetism and Aeronomy. These are the data formerly published in the Journal of Geophysical Research. They are now, however, grouped by the storm rather than by station. The geomagnetic latitude of the station is indicated. The beginning time is given to the hour and minute in UT. The ending time is given only to the nearest hour. This is the time of cessation of reasonably marked disturbance movements in the trace. More specifically, the time when the K-index measure has diminished to 2 or less for a reasonable period.

The type of sudden commencement, if any, together with its magnitude in each element D, H or Z is next in the table: sc = sudden commencement; sc* = small initial impulse followed by main impulse (in this case the amplitude is that of the main pulse only, neglecting the initial brief pulse); dots in these columns represent a storm with gradual commencement; dashes indicate no data entries. Signs of amplitudes of D and Z are taken algebraically; D reckoned positive if toward the east and Z reckoned positive if vertically downward. The storm is classified as moderate (m) if an individual K index reaches 5, as moderately severe (ms) if K index 6 or 7 is reached, and as severe (s) if K index 8 or 9 is reached. In the next columns the day and the three-hour periods on that day when the K index reached its maximum are given. Finally, in the last three columns the maximum ranges in D, H and Z during the storm are given.

The storm grouping (by number in the final column) is arbitrary. Especially if gradual commencement storms are involved, there can be a considerable spread in the days included. In some cases a single number has been assigned though beginning times occur on two or more consecutive dates. For each date the data are listed in north-to-south geomagnetic latitude order. The table on page 51 gives the abbreviations used for the observatory names.

RADIO PROPAGATION QUALITY INDICES

One can take as the definition of a radio propagation quality index: the measure of the efficiency of a medium-powered radio circuit operated under ideal conditions in all respects, except for the variable effect of the ionosphere on the propagation of the transmitted signal. The indices given here are derived from monitoring and circuit performance reports, and are the nearest practical approximation to the ideal index of propagation quality.

Quality indices are expressed on a scale that ranges from one to nine. Indices of four or less are generally taken to represent

significant disturbance. (Note that for geomagnetic K-indices, disturbance is represented by high numbers.) The adjectival equivalents of the integral quality indices, known as the CRPL quality figure scale, are as follows:

1 = useless	4 = poor-to-fair	7 = good
2 = very poor	5 = fair	8 = very good
3 = poor	6 = fair-to-good	9 = excellent

The forecasts are expressed on the same scale. The tables summarizing the outcome of forecasts include categories P-Perfect; S-Satisfactory; U-Unsatisfactory; F-Failure. The following conventions apply:

P - Forecast quality equal to observed.

S - Forecast quality one grade different from observed.

U - Forecast quality two grades or more different from observed when both forecast and observed were ≥ 5, or both ≤ 5.

F - Other times when forecast quality two or more grades different from observed.

Full discussion of the reliability of forecasts requires consideration of many factors besides the over-simplified summary given.

The quality figures represent a consensus of experience with radio propagation conditions. Since they are based entirely on monitoring or traffic reports, the reasons for low quality are not necessarily known and may not be limited to ionospheric storminess. For instance, low quality may result from improper frequency usage for the path and time of day. Although, wherever it is reported, frequency usage is included in the rating of reports, it must often be an assumption that the reports refer to optimum working frequencies. It is more difficult to eliminate from the indices conditions of low quality for reasons such as multipath or interference. These considerations should be taken into account in interpreting research correlations between the Q-figures and solar, auroral, geomagnetic or similar indices.

North Atlantic Radio Path -- The CRPL quality figures, Qa, are compiled by the Telecommunications Disturbance Forecast Center at Fort Belvoir, Virginia, from radio traffic data for North Atlantic transmission paths closely approximating New York-to-London. These are reported by the Canadian Defence Research Board, Canadian Broadcasting Corporation, and the following agencies of the U. S. Government: Coast Guard, Navy, Army Communications Center, U. S. Information Agency. Supplementing these data are ESSA monitoring, direction-finding observations and field-strength measurements of North Atlantic transmission made at Fort Belvoir.

The original reports are submitted on various time intervals. The observations for each 6-hour interval are averaged on the original scale. These 6-hour indices are then adjusted to the 1 to 9 quality-figure scale by a conversion table prepared by comparing the distribution of these indices for at least four months, usually a year, with a master distribution determined from analysis of the reports originally made on the 1 to 9 quality-figure scale. A report whose distribution is the same as the master is thereby converted linearly to the Q-figure scale. The 6-hourly quality figure is the mean of the reports available for that period.

The 6-hourly quality figures are given in this table to the nearest one-third of a unit, e.g., 5o is 5 and 0/3; 5- is 4 and 2/3; 5+ is 5 and 1/3. Other data included are:

(a) Whole-day radio quality indices, which are averages of the four 6-hourly indices.

(b) Short-term forecasts, issued every six hours by the North Atlantic Radio Warning Service. These are issued one hour before 00^h, 06^h, 12^h, 18^h, UT and are applicable to the period 1 to 7 hours ahead.

(c) Advance forecasts (CRPL-Jc) are issued once a week and are applicable to 1 to 7 days ahead for HF radio propagation conditions on typical high latitude paths passing through or near the auroral zone. They are scored against the average of the whole day North Atlantic and North Pacific quality figures. They are modified as necessary by one of two types of the Special Disturbance Warnings applicable 1 to 6 days ahead (CRPL-SDW or CRPL-Jc supplement).

(d) Half-day averages of the geomagnetic K indices measured by the Fredericksburg Magnetic Observatory of the U. S. Coast and Geodetic Survey, K_{Fr}.

(e) Predictions of the daily A-index for Fredericksburg, A_{Fr}, issued weekly applicable to 1 to 7 days ahead, are compared with the observed A_{Fr}.

North Pacific Radio Area -- The CRPL radio propagation quality for the North Pacific Area, Qp, is compiled by the ESSA Space Disturbance Monitoring Station at Anchorage, Alaska from measurements made at the station of signal-to-noise ratios on the following circuits: Adak-to-Anchorage on 10 MHz and 5 MHz, and Tokyo-to-Anchorage on 15 MHz. Each circuit identifies itself every half-hour and during this short period the signal drops to the noise level of the

path. The circuits are calibrated in dbm (decibels below 1 milliwatt) and the values scaled, for each hour, are the differences in db between the median signal level and the median noise level. This is the signal-to-noise value.

Predictions of signal-to-noise for undisturbed conditions on each path are made available by the Ionospheric Telecommunications Laboratory, Frequency Utilization Section in Boulder, Colorado. The actual daily values on each path are compared with these predicted values and this comparison is then used to decide whether conditions are normal or otherwise. The following five classifications describe the radio propagation quality with respect to the predicted normal values:

N++	Conditions giving more than 15db above predicted signal-to-noise values (considered as $Q \geq 8$).
N+	Conditions giving between 5db and 15db above predicted signal-to-noise values (considered as $Q = 7$).
No	Conditions within 5db of the predicted signal-to-noise values (considered as $Q = 6$).
N-	Conditions giving between 5db and 15db below predicted signal-to-noise values (considered as $Q = 5$).
N--	Conditions giving more than 15db below predicted signal-to-noise values (considered as $Q \leq 4$).

The hourly values are combined to give the 6-hourly and whole day values that are found in the table. The half-day averages of the geomagnetic K indices and the daily A-index measured by the Sitka, Alaska Magnetic Observatory of the U. S. Coast and Geodetic Survey, K_{Si} and A_{Si} are given.

Forecasts of HF propagation conditions for the North Pacific are no longer made at the Anchorage station. There is a local tape-recorded service, telephone (area code 907) 277-3355 giving a statement of current magnetic conditions, a forecast of geomagnetic conditions for the coming day, current ionospheric conditions, a radio propagation quality figure for the past 24 hours and a predicted figure for the next 24 hours, predicted in-out time for

various operational radio circuits and a report of special events, if any, such as abnormal D region absorption.

Comparison Charts -- A chart compares the North Atlantic short-term forecasts with the 6-hourly Qa-figures. A second chart compares the outcome of the high latitude advance forecasts with a type of "blind" forecast. For the latter, the frequency for each quality grade, as determined from the distribution of quality grades in the four most recent months of the current season, is partitioned among the grades observed in the current month in proportion to the frequencies observed in the current month.

Transmission Frequency Ranges -- Ranges of useful frequencies between 2 and 26 MHz on the North Atlantic radio path are shown in a series of diagrams one for each day. The shaded area indicates the range of frequencies for which transmissions of S meter readings 3 or greater were observed equal to a field strength of ≥ 0.4 μV/m. This value corresponds roughly to the lower limit of satisfactory MUX operation between commercial stations using directional antennas. (For data through December 1966 the range for S meter readings 5 or greater equal to 6 μV/m was given). The blacker the diagram, the quieter the day has been: a narrow strip indicates either high LUHF, low MUF, or both.

These diagrams are based on data reported to ESSA by the German Post Office through the Fernmeldetechnisches Zentralamt, Darmstadt, Federal Republic of Germany, being observations every one and a half hours of selected transmitters located in the eastern portion of U.S.A. north of 39° latitude, as received at Lüchow 53.0°N, 11.2°E. (Before December 1, 1966 the observations were made near Detmold, 51.6°N, 8.9°E. Before January 6, 1958, transmitters located south of 39° latitude were also included. The magnetic activity index, A_{Fr}, from Fredericksburg, Virginia, is also given for each day.

DATA FOR SIX MONTHS BEFORE MONTH OF PUBLICATION
TABLE OF CONTENTS

SOLAR FLARES

This table presents grouped and averaged solar-flare data for the month preceding publication by six months. Various reports that pertain to the same flare are listed together (see pages 12 to 16 for detailed description of entries) headed by a summary "group report" that gives average values for each measured quantity and, under "REMARKS," the number of observatories reporting the flare, the number of values entering the average importance, and the number entering the average measured area. The grouping and averaging are done by an electronic computing machine. The rules are changed from time to time, so that these data should be regarded as current results of an experiment in data processing, rather than as homogeneous, carefully edited records. The principal criteria for grouping reports together are position and time of maximum. Each maximum time reported by two or more observatories forms the basis of a group description, but a single group number may be assigned to several group reports when they are considered to describe successive maxima of a single flare. For each observatory that saw the maximum phase of the flare a single set of values is included in the average values describing that maximum. In some months the averages represent normalized values, obtained by correcting each reported value of importance and of measured area by an amount that depends on the reported value, the position of the flare on the solar disk, and the reporting observatory. Intervals when no observatory reported patrolling the sun are listed chronologically in the table and also shown graphically for the observatories that submit reports of patrol times.

SOLAR X-RAY RADIATION

NRL - Satellites OSO-4 and OGO-4 -- The solar x-ray emission data from the NRL x-ray monitoring satellites are here presented in a graphic form. These data are generally plotted one point per reception by a tracking station. More points, however, are plotted if there is a considerable variation. Overlapping points have been removed when adjacent stations receive the same values. These plots are prepared in half-month intervals. Satellite 1965-93A ceased operation in November 1967. Data from OSO-4 (1967-100A) and OGO-4 (1967-73A) are currently being given.

McMath-Hulbert Observatory - OSO-3 -- The McMath-Hulbert Observatory soft solar x-ray detector on OSO-3 provides values of the x-ray flux in the wavelength range 8-12 Angstroms. Data are acquired during a 24-hour day on a duty cycle of about one hour daylight observation followed by about a half-hour of satellite night. At the present time about one-third of the observations have been reduced in preliminary form.

Solar x-ray fluxes are computed assuming that the flux distribution corresponds to a 2×10^6 degree K "grey body". They are given as E(8,12) ergs cm^{-2} sec^{-1} for the wavelength range 8-12 Angstroms, and are not corrected for variation of the earth-sun distance during a year. The fluxes E(8,12) may be converted to the 8-20 Angstrom flux by multiplying the former by the factor 3.84. The absolute calibration of the McMath-Hulbert instrument is thought to be within $\pm$6% of correct. Its stability in orbital operation is about $\pm$1%. There is an additional 1% uncertainty in flux values caused by coupling of satellite spin rate with amplifier frequency response.

The column entries in the table are explained below:

Observing times for data thus far reduced in preliminary form are listed for each day in the first table. For each observing interval the lowest E(8,12) reached is given. Usually the soft x-ray flux is quite variable. An attempt to describe the nature of variations observed is made in the Remarks column. Generally, only those fluctuations with amplitude ≥ 0.002 ergs cm^{-2} sec^{-1} are described.

Small corrections to the values of E(8,12), of the order of a few percent, are not yet introduced into these data.

In a second table outstanding events which occurred during the observing hours of the table described above are listed. Only those events for which the observed flux increase was ≥ 0.005 ergs in cm^{-2} sec^{-1} are given. The table includes for each event approximate time of beginning, maximum and ending, and fluxes at beginning and maximum in the event (where observed). Times are correct to $\pm$2 or 3 minutes, while small flux corrections of the order of a few percent have not yet been introduced into these data.

The detector measures x-ray fluxes in discrete steps. Up to flux values of E(8,12) $\simeq$ 0.0044 ergs cm^{-2} sec^{-1}, the interval between steps is about 0.000035 ergs cm^{-2} sec^{-1}. Above E(8,12) $\simeq$ 0.0044, the interval between steps is about 0.00095. The instrument saturates at E(8,12) $\simeq$ 0.12 ergs cm^{-2} sec^{-1}.

University of Iowa - Explorer 33 -- Three mica-window neon-filled Geiger tubes on the satellite Explorer 33 are used to monitor soft x-ray emission of the whole disc of the sun. (See J. A. Van Allen and N. F. Ness, J. Geophys. Res., 72, 935-942, 1967, for fuller description of the apparatus.) The observations began on 1 July 1966 and provide one measurement each 81.8 seconds essentially continuously, with the exception of four 20-day periods per year during which no one of the three detectors views the sun. The absolute photon efficiency and the absolute energy flux efficiency for an x-ray beam parallel to the axis of the detector are shown in Figures 1 and 2, respectively. A geometric obliquity factor $f(\alpha)$ has been determined experimentally for each detector as a function of the angle α between the spin axis of the satellite and the satellite-sun line. The application of this factor and Figure 2 converts the counting rate of a detector to absolute energy flux units (ergs/cm^{2}sec) for any assumed spectral distribution. Sensitivity of the detectors is typically about 2×10^{-6} ergs/cm2sec ($2 < \lambda < 12$ A°) and the dynamic range is 10^5.

The detectors are insensitive to solar ultraviolet.

The present listing of x-ray flares is independent of $f(\alpha)$ since the flares are characterized by a ratio of peak intensity to that of the ambient quiet sun. Continuous plots of all data are available.

The listings will be continued for the useful life of the satellite which is already known to exceed one year. For each event the time of onset (UT), time of maximum (UT), and peak ratio to quiet sun value existing before burst occurs are given together with appropriate remarks.

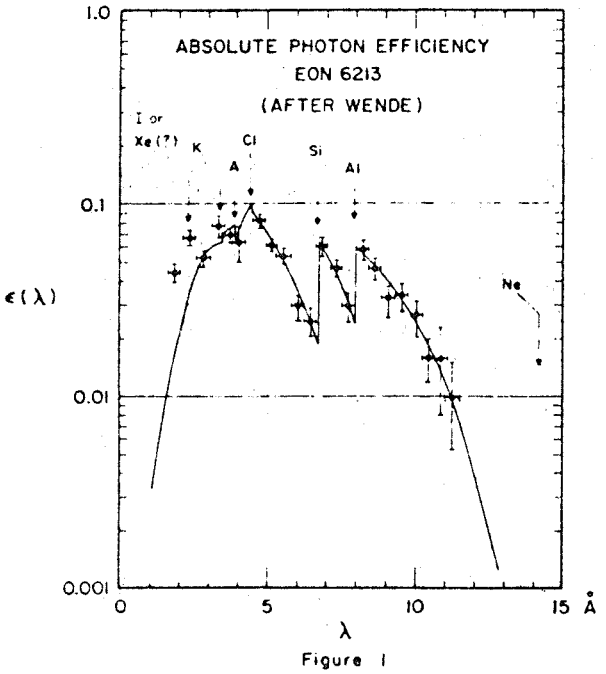

Figure 1

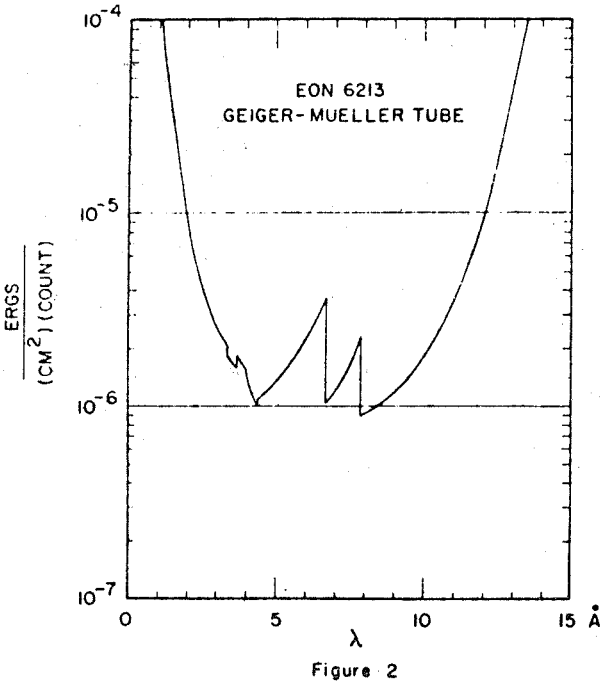

Figure 2

SOLAR PROTON MONITORING

The Solar Proton Monitoring Experiment (SPME) is a joint effort by C. O. Bostrom of the Johns Hopkins University Applied Physics Laboratory and by D. J. Williams and J. F. Arens of the NASA Goddard Space Flight Center. The personnel listed above are those responsible for the construction, spacecraft integration, (JHU/APL) and calibration (GSFC) of the experiment and the data reduction, handling and presentation (GSFC) of the monitor data. The initial conception, design, and proposal of the SPME were carried out by C. O. Bostrom, D. J. Williams, D. E. Hagge and F. B. McDonald.

The SPME was successfully launched May 24, 1967 aboard the NASA Explorer 34 (IMP F) satellite. Similar equipment is scheduled for launch aboard satellites IMP G and I.

The primary purpose of the SPME is to provide systematic monitoring of solar cosmic rays over at least half a solar cycle. The basic requirements set forth for such a monitoring program were:

1) to furnish simple reliable flux and spectral measurements,

2) to operate over a wide flux range and in particular provide coverage for very large events,

3) to provide a simple and easily reproducible detector system to form the basis of an operational monitoring program.

The SPME satisfies the above requirements. Data from the experiment are now being made available to the scientific community through this monthly bulletin.

The SPME consists of an array of solid state detectors designed to measure proton intensities in the following energy ranges $E_p \geq 10$ Mev, $E_p \geq 30$ Mev, and $E_p \geq 60$ Mev.

Since the overall design goal was to obtain a standard, reliable and easily reproducible detection scheme specifically aimed at monitoring solar cosmic rays, the method chosen was to use separate detectors for each energy range and to employ combinations of discriminator levels and shielding thicknesses to define the energy response of each channel. Such a method allows for accurate absolute flux determinations and for unit to unit comparisons when using a series of payloads to monitor the solar flux over an extended time period ($\geq$ 0.5 solar cycles).

The following table indicates the SPME response to alpha particles which will introduce an ambiguity in the solar proton flux observations. To estimate the size of this uncertainty reproduced as Figure 1 is Figure 29-5 from Fichtel (Part 29, Proceedings of "AAS-NASA Symposium

on the Physics of Solar Flares", Oct. 1963, edited by W. N. Hess, NASA SP-50, which shows the proton to helium nuclei ratio observed during 1960 as a function of energy per nucleon. From this figure it is seen that a maximum uncertainty of ~ 10% may be expected due to the alpha particle flux at the energies shown in Figure 1.

Proton and Alpha Particle Energy Sensitivities of SPME

Channel	E_p	E_α
1	≥ 60 Mev	≥ 240 Mev
2	≥ 30 Mev	≥ 120 Mev
3	≥ 10 Mev	≥ 40 Mev

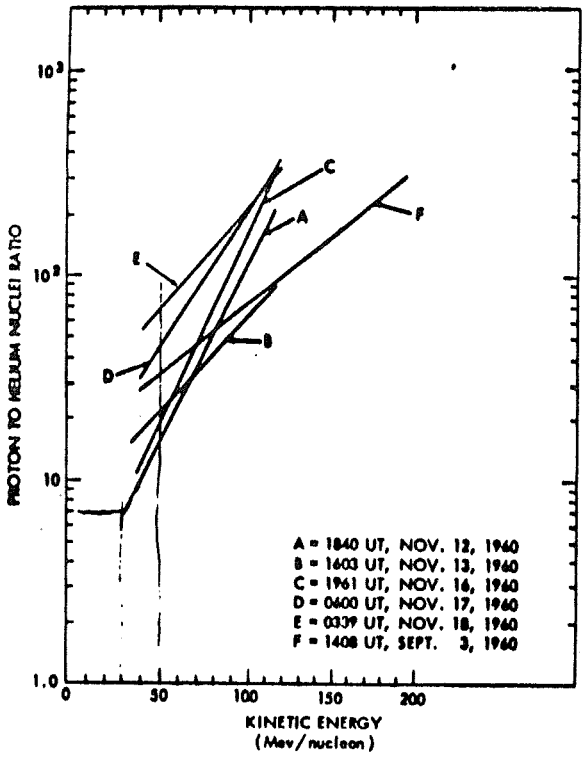

Figure 1

A more detailed description of the detectors follows.

Channel 1 ($E_p \geq 60$ Mev) and Channel 2 ($E_p \geq 30$ Mev):

Each of these two higher energy channels consists of three solid state detectors mounted on orthogonal axes and surrounded by a hemispherical shield. Figure 2 shows the assembly of these units. This arrangement is a straightforward method of obtaining a large area and a relatively smooth geometric factor when using disk shaped detectors.

The shielding thickness is by far the most important factor in determining the energy threshold in this particular arrangement. The thicknesses used are 5.6 mm Cu and 1.6 mm Cu and are indicated in Figure 2.

The detectors used in this assembly are surface barrier solid state detectors, fully depleted, 700 microns thick, having a usable surface area of 0.83 cm^2 and a noise level nominally $<$ 20 kev at the operating bias voltage. These units fully deplete at $<$ 150 volts and are operated at 200 volts.

The three detector outputs are fed in parallel to a preamp-amplifier-discriminator package and thence to the data processing electronics. Three 20 kev detectors yield a total detector noise level of $\sim$ 35 kev in channels 1 and 2. This coupled with a preamp noise level of 25 kev yields a measured total system noise level of $\sim$ 40 kev.

At minimum ionizing energies, the proton energy loss in 700μ of silicon is $\sim$ 280 kev. A discriminator bias level of 150 kev is both well below the minimum ΔE_p of 280 kev and well above the system noise level of 40 kev. The 150 kev discriminator level causes but a negligible shift of the energy threshold ($<$ 10 kev). Also, the response of the unit is relatively independent of discriminator level shifts.

Due to the high bias levels, the shielding thicknesses and mode of operation radiation damage effects will be negligible for several years for channels 1 and 2.

Channel 3 ($E_p \geq 10$ Mev):

This detector consists of a 3 mm cubic Li drifted solid state detector surrounded by a 170 mg/cm^2 (0.63 mm) Al shield. Figure 3 is a diagram of this unit.

The detector has a noise level of $<$ 50 kev at its operating bias of 200 volts. The discriminator level of 300 kev will raise the energy threshold $\sim$ 25 kev. Radiation damage effects in channel 3 will be negligible for at least a year.

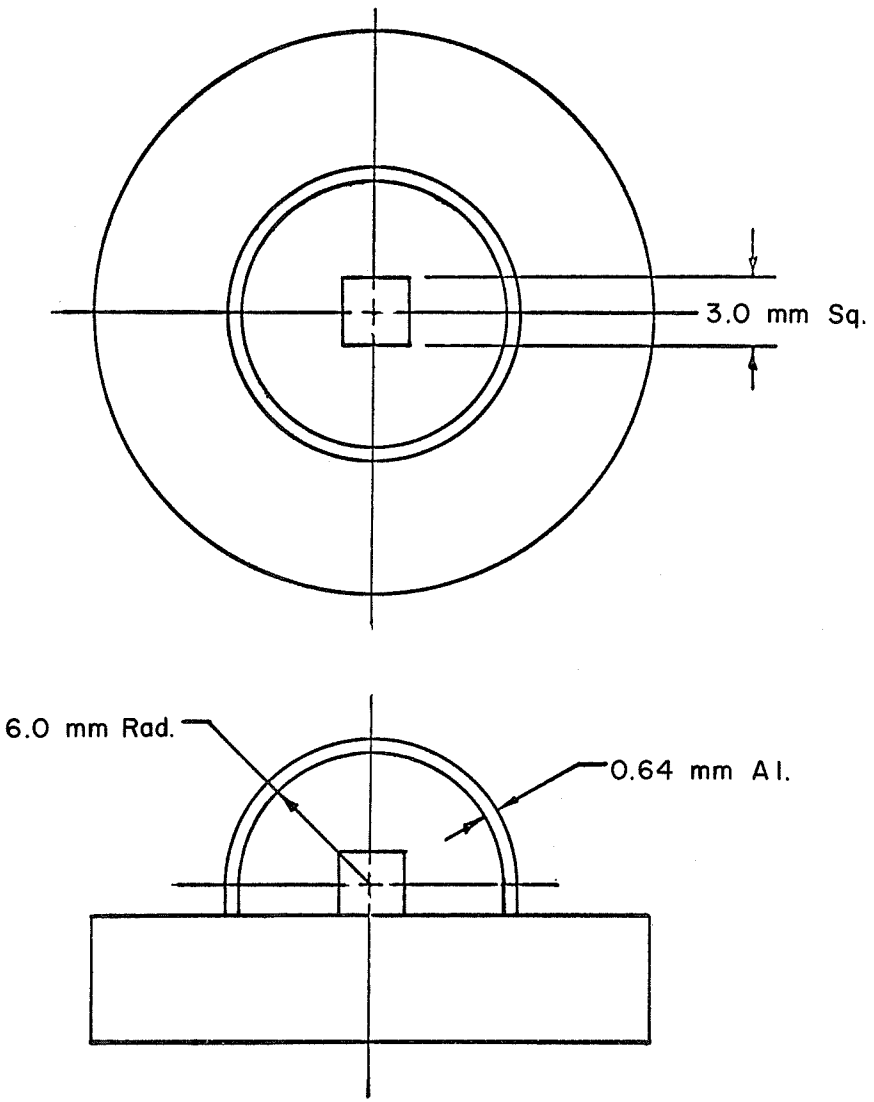

SCALE 4:1

Figure 2

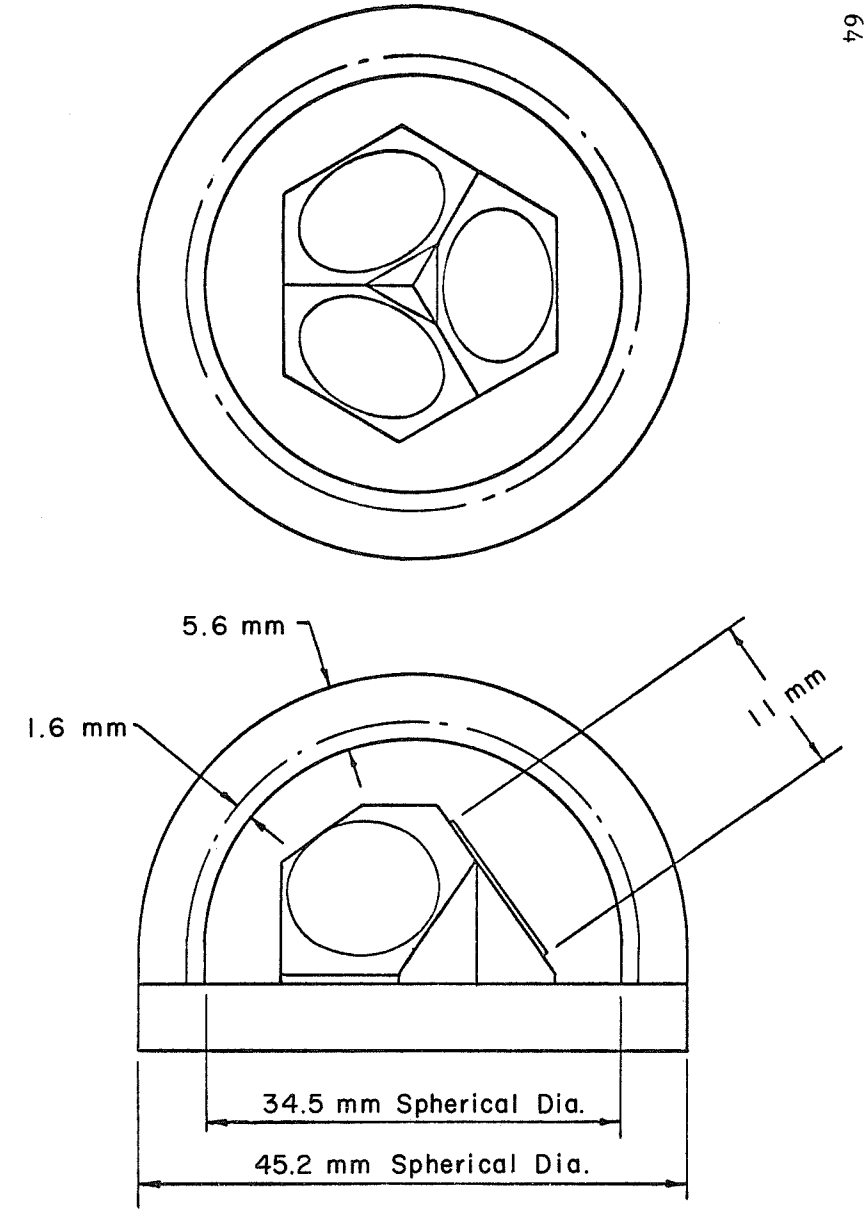

SHIELDING MATERIAL-COPPER

Figure 3

All data from the SPME published as monitoring data satisfy the following requirements:

1) final orbit determinations have been made

2) final time corrections have been made

3) all data quality flags indicate that the individual data point is "good"

Data that satisfy these requirements are then used to construct hourly averages of the respective energy channels. The ≥ 60 Mev and ≥30 Mev channels are sampled for 19.2 seconds once every 2 minutes 43.8 seconds. The ≥ 10 Mev channel is sampled twice every 2 minutes 43.8 seconds at 19.2 seconds per sample. Thus the maximum number of points in an hourly average is 22 for the ≥ 60 Mev and ≥ 30 Mev channels and 44 for the ≥ 10 Mev channel. If the number "good" data points is less than 5 the hourly average is not constructed.

These hourly averages are then tabulated in a grid where the hours of the day run to the right and the days of the month run from top to bottom. The day is identified as both day of the month and day of the year. The published listing should be essentially self-explanatory.

The hourly averages are also plotted vs. time in monthly blocks. The plots of hourly averaged fluxes for the various channels should also be self-explanatory. The two plots below the plot of flux values are included to show the satellite position in orbit at the time of the flux measurement. The lower plot is simply a projection of the orbit on the ecliptic plane with the lower circle representing the earth and the upper circle the sun. Apogee is at a radial distance of $\sim$ 34 earth radii and during September 11, 1967 the semi major axis of the orbit projected to the earth-sun line (see the plot for September 1967).

The middle plot (which resembles a fully rectified sine wave) shows the radial distance to satellite as a function of time. At the cusps, the satellite is at perigee and at the crests the satellite is at apogee, $\sim$ 34 R_E. The vertical scale is linear. Note the response of the detectors to the radiation belts at perigee; this shows up very clearly in the ≥ 10 Mev channel and is usually but a single high point for the ≥ 60 Mev and ≥ 30 Mev channel.

The flux values listed and plotted are accurate to $\pm$ 25% for the ≥ 60 Mev and ≥ 30 Mev channels and to $\pm$ 50% for the ≥ 10 Mev channel only during the times of solar cosmic ray events.

The directional factor becomes more nearly 4π for galactic cosmic rays due to their much higher characteristic energy. Therefore the background fluxes which are due to galactic cosmic rays, are incorrect as shown on the plots. These have not been corrected because more accurate start times and initial fluxes for solar events may be obtained if the detector response is seen to rise from its own background.

The $\geq$ 60 Mev and $\geq$ 30 Mev channels indicate a similar background flux whereas the $\geq$ 10 Mev channel shows a slightly different background flux value. This is due to differences in i) edge effects in a cube versus disc detector and, ii) differences in satellite shielding. These effects are more important at galactic cosmic ray energies than at the solar cosmic ray energies of this experiment.

DATA FOR

MISCELLANEOUS TIME PERIODS

POLAR CAP ABSORPTION EVENTS

A list of principal polar cap absorption (PCA) events will be published at approximately six month intervals. The list will include events where the equivalent 30 MHz absorption exceeded 1 db on a polar riometer, though events of smaller magnitude will be included if they are considered to be adequately verified as PCA.

Although the riometer is not the most sensitive technique for detecting solar-proton bombardment, it has been chosen as the source of this list on the basis of its long history and general acceptance as a standardized technique for observing PCA events. It has the added advantage over most other indirect techniques of supplying essentially continuous quantitative measurements throughout the entire course of a PCA event.

While the riometer is sensitive to ionization by solar protons in the entire energy range from below 1 Mev to more than 100 Mev, most of its effective response is to energies in the 10 to 30 Mev range. The time history of a PCA event recorded by a high-latitude riometer thus probably represents the time history of solar protons in this energy range of the earth. The arbitrary lower limit of 1 db recorded by a 30 MHz riometer corresponds roughly to a flux of 16 protons cm^{-2} sec^{-1} $ster^{-1}$ greater than 14 Mev for an 'average' proton spectrum, and the flux for other values of absorption is roughly proportional to the square of the absorption.

The table of events will include the following information:

a) start time in UT of the PCA;
b) maximum absorption and approximate time in UT of the peak of the event;
c) identification of the probable flare, including information on Type IV noise storms recorded by the riometers themselves;
d) and parameters of the associated magnetic storms.

Sources for riometer data will include the polar riometers operated by the Space Disturbances Laboratory, ESSA, and published data from other groups operating riometers.

RETROSPECTIVE WORLD INTERVALS

At the times Retrospective World Intervals are announced by the International Ursigram and World Days Service, these will be presented in this section.

OTHER DATA

Information available either annually or on a non-routine publication basis will be given. The descriptive material necessary to understand the data will be included in the issue presenting the data.

A C K N O W L E D G E M E N T S

These monthly reports would not be possible without the continuing support and cooperation of scientists throughout the world. Much of the data included have been obtained through either the International Ursigram and World Days Service program or the international exchange of geophysical observations between World Data Centers in accordance with the principles set forth in recommendations of relevant organizations of the International Council of Scientific Unions.

Special thanks are due to many individuals including the following:

Name	Organization	Data Type
R. H. Davis	American Association of Variable Star Observers	Sunspots, SID
P. S. McIntosh	Space Disturbances Laboratory, ESSA	Sunspots, Hα photographs
M. Waldmeier	Swiss Federal Observatory	Sunspots
H. Dodson Prince	McMath-Hulbert Observatory	Calcium plages, flares, SID
R. Howard	Mount Wilson Observatory	Magnetic classifications of sunspots, magnetograms
J. W. Evans	Sacramento Peak Observatory	Flares, coronal indices
A. A. Giesecke	Instituto Geofisico del Peru	SID
R. G. Giovanelli	CSIRO Division of Physics, Sydney, Australia	Flares
J. J. Hennessey	Manila Observatory	Flares, SID
J. T. Jefferies	Hawaii Institute of Geophysics	Flares, solar noise, SCNA, SEA
Y. Ohman	Anacapri Swedish Observatory	Flares
H. Ramsey	Lockheed Observatory	Flares
C. Sawyer	Space Disturbances Laboratory, ESSA	Flares

Name	Organization	Data Type
R. N. Bracewell	Stanford University	Solar Noise
J. P. Castelli	USAF Cambridge Research Laboratories	Solar Noise
W. N. Christiansen	University of Sydney	Solar Noise
A. E. Covington	National Research Council, Canada	Solar Noise
L. B. Craine	Washington State University	Solar Noise
J. P. Hagen	Pennsylvania State University	Solar Noise
W. K. Klemperer	Space Disturbances Laboratory, ESSA	Solar Noise
A. R. Maxwell	Harvard Radio Astronomy Station Fort Davis, Texas	Solar Noise
M. Pick	Meudon Observatory	Solar Noise
J. W. Warwick	University of Colorado	Solar Noise
J. P. Wild	CSIRO Division of Physics, Sydney, Australia	Solar Noise
J. H. Wolfe	NASA Ames Research Center	Solar wind velocities
D. B. Bucknam	Space Disturbances Forecast Center, ESSA	Solar proton events
H. L. DeMastus	Sacramento Peak Observatory	Hα photographs
	Cable and Wireless, Ltd.	SID
S. Maagoe	ESSA Space Disturbance Monitoring Station, Anchorage, Alaska	SID, radio quality figures
R. F. Donnelly	Space Disturbances Laboratory, ESSA	SFD
T. Fortini	Mount Mario Observatory, Rome	SID
A. G. Jean	ESSA, Space Disturbances Laboratory	SID

Name	Organization	Data Type
S. Katahara	NBS, Maui Station	SPA
A. P. Mitra	National Physical Laboratory, India	SID
P. C. Yuen	University of Hawaii	SFD
R. W. Kreplin	U. S. Naval Research Laboratory	Solar X-rays
R. G. Teske	McMath-Hulbert Observatory	Solar X-rays
J. A. Van Allen	University of Iowa	Solar X-rays
H. Carmichael	Atomic Energy of Canada, Ltd.	Cosmic rays
K. G. McCracken	Graduate Research Center of the Southwest, Dallas, Texas	Cosmic rays
J. A. Simpson	University of Chicago	Cosmic rays
M. Siebert	Göttingen University, G.F.R.	Magnetic Indices
D. Van Sabben	Meteorological Office, DeBilt, Holland	Magnetic Indices
B. Beckmann	Fernmeldetechnisches Zentralamt, Darmstadt G.F.R.	Radio quality figures
E. J. Wiewara	ESSA's Telecommunications Disturbance Forecast Center, Ft. Belvoir, Va.	Radio quality figures
C. O. Bostrom	Johns Hopkins University Applied Physics Laboratory	Solar Protons
D. J. Williams J. F. Arens	NASA Goddard Space Flight Center	Solar Protons
G. C. Reid F. H. Leinbach	Space Disturbances Laboratory, ESSA	PCA

INDEX FOR

SOLAR-GEOPHYSICAL DATA

On the following pages will be found the serial number of the report or reports in which data of a given type for any given month will be found, beginning with data for July 1957 through December 1967.

STONYHURST DISKS

Two transparencies provide Stonyhurst disks in the size of several of the solar maps or drawings presented in the second section of these monthly reports.

INDEX FOR IGY DATA PUBLISHED IN CRPL-F Part B

	1957						1958											
	Jul	Aug	Sep	Oct	Nov	Dec	Jan	Feb	Mar	Apr	May	Jun	Jul	Aug	Sep	Oct	Nov	Dec
American Relative Sunspot Numbers R_A'	157	158	159	160	161	162	163	164	165	166	167	168	169	170	171	172	173	174
Zurich Provisional Relative Sunspot Number R_Z	156	157	158	159	160	161	162	163	164	165	166	167	168	169	170	171	172	173
Zurich Final Sunspot Numbers R_Z	166	166	166	166	166	166	175	175	175	175	175	175	175	175	175	175	175	175
2800 Mc - Daily Values of Solar Flux (Ottawa)	156	157	158	159	160	161	162	163	164	165	166	167	168	169	170	171	172	173
Calcium Plage and Sunspot Regions	156	157	158	159	160	161	162	163	164	165	166	167	168	169	170	171	172	173
Coronal Line Emission Indices	156	157	158	159	160	161	162	163	164	166	166	167	168	169	170	171	172	173
			165	165	165	165	165	171	171	171	171	171	171					
							171											
Optical Observations Flares	156	157	158	159	160	161	162	163	164	165	166	167	168	169	170	171	172	173
	166	167	168	168	169	169	170	170	171	171	172	172	173	173	174	174	175	175
	169	174	174	174	161	174	174		174	174	174					176		
	174		175		174													
Flare Patrol Observations	158	158	158	159	160	161	162	163	164	165	166	167	168	169	170	171	172	173
	166	167	168	168	169	169	170	170	171	171	172	172	173	173	174	174	175	175
	176	176	176	176	176	176	176	176	176	176								
Subflares	156	157	158	160	161	162	163	164	165	166	167	168	169	170	171	172	173	174
Ionospheric Effects (SWF)	157	158	159	160	161	162	163	164	165	166	167	168	169	170	171	172	173	174
Ionospheric Effects (SCNA-SEA-Bursts)									171	172	173	174	175	176	177	178	178	179
9530 Mc-Daily Data & Outstanding Occurrences (USNRL)								176	175	174	172	170	170	170	170	171	172	173
3200 Mc-Daily Data & Outstanding Occurrences (USNRL)								176	175	174	172	170	170	170	170	171	172	173
2800 Mc-Outstanding Occurrences (Ottawa)	156	157	158	159	160	161	162	163	164	165	166	167	168	169	170	171	172	173
2800 Mc-Hours of Observations (Ottawa)	158	158	158	161	161	161	164	164	164	167	167	167	170	170	170	173	173	173
470 Mc-Daily Data (Boulder)	156	157	158	159	161	162	163	164	165									
470 Mc-Outstanding Occurrences (Boulder)	156	157	159	159	161	162	163	164	165									
200 Mc-Daily Data (Cornell)	156	157	158	159	160	161	163	163	164	165	167	167	168	169	170	171	172	173
200 Mc-Outstanding Occurrences (Cornell)	156	157	158	159	160	161	163	163	164	165	167	167	168	169	170	171	172	173
169 Mc-Interferometric Observations (Nançay)	171	171	171	171	171	171	171	171	171	171	171	171	171	171	171	171	172	173
167 Mc-Daily Data (Boulder)	156	157	158	159	162	162	163	164	165	167	168	169	170	172	173	174	175	176
167 Mc-Outstanding Occurrences (Boulder)	156	157	159	159	162	162	163	164	165	168	169	169	170	172	173	174	175	176
100-580 Mc-Spectrum Observations (Ft. Davis)												174	168	169	170	171	172	174
Geomagnetic Indices C, K_p, A_p, - Selected Days	157	158	159	160	161	162	163	164	165	166	167	168	169	170	171	172	173	174
27-day Charts of K_p Indices for Year	174	174	174	174	174	174	174	174	174	174	174	174	174	174	174	174	174	174
NARWS - CRPL Quality Figures & Forecasts	157	158	159	160	161	162	163	164	165	166	167	168	169	170	171	172	173	174
NARWS - Comparison Graphs	157	158	159	160	161	162	163	164	165	166	167	168	169	170	171	172	173	174
NARWS - Graphs of Useful Frequency Ranges	157	159	159	160	161	162	163	164	165	166	167	168	169	170	171	172	173	174
NPRWS - CRPL Quality Figures & Forecasts	157	158	159	160	161	162	163	164	165	166	167	168	169	170	171	172	173	174
NPRWS - Comparison Graphs	157	158	159	160	161	162	163	164	165	166	167	168	169	170	171	172	173	174
Alert and SWI Decisions	158	158	158	159	160	161	162	163	164	165	165	167	168	168	170	171	172	173
										166	166			169				

INDEX FOR IGC DATA PUBLISHED IN CRPL-F Part B

	1959 Jan	Feb	Mar	Apr	May	Jun	Jul	Aug	Sep	Oct	Nov	Dec
American Relative Sunspot Numbers R_A'	175	176	177	178	179	180	181	182	183	184	185	186
Zurich Provisional Relative Sunspot Number R_Z	174	175	176	177	178	179	180	181	182	183	184	185
Zurich Final Sunspot Numbers R_Z	187	187	187	187	187	187	187	187	187	187	187	187
2800 Mc-Daily Values of Solar Flux (Ottawa)	174	175	176	177	178	179	180	181	182	183	184	185
Calcium Plage and Sunspot Regions	174	175	176	177	178	179	180	181	182	183	184	185
Coronal Line Emission Indices	174	175	176	177	178	179	180	181	183	183	184	185
										185	185	
Optical Observations Flares	174	175	176	177	178	179	180	181	182	183	184	185
	176	178	179	180	181	182	183	184	185	186	187	188
	178	185	185	185	185	185	185	185			191	189
	185											191
Flare Patrol Observations	174	175	176	177	178	179	180	181	182	183	184	185
	176	178	179	180	181	182	183	184	185	186	187	188
	178	185	185	185	185	185	185	185			191	191
	185											
Subflares	175	176	177	178	179	180	181	182	183	184	185	186
Ionospheric Effects (SWF)	175	176	177	178	179	180	181	182	183	184	185	186
Ionospheric Effects (SCNA-SEA-Bursts)	180	181	182	183	184	184	184	185	186	187	187	188
9530 Mc-Daily Data & Outstanding Occurrences (USNRL)	174	175	176	177								
3200 Mc-Daily Data & Outstanding Occurrences (USNRL)	174	175	176	177								
2800 Mc-Outstanding Occurrences (Ottawa)	174	175	176	177	178	179	180	181	182	183	184	185
2800 Mc-Hours of Observation (Ottawa)	176	176	176	179	179	179	182	182	182	185	185	185
200 Mc-Outstanding Occurrences (Hawaii)						180	182	185				
169 Mc-Interferometric Observations (Nançay)	174	175	176	177	178	179	180	181	182	183	184	185
167 Mc-Outstanding Occurrences (Boulder)	176	177	178	178	179	180	180	181	182	183	184	185
167 Mc-Hours of Observation (Boulder)	182	182	182	182	182	182	182	182	182	183	184	185
25-580 Mc-Spectrum Observations (Ft. Davis)	182	182	182	184	184	184	188	188	188	192	192	192
Geomagnetic Indices C, K_p, A_p, - Selected Days	175	176	177	178	179	180	181	182	183	184	185	186
27-Day Charts of K_p Indices for Year	186	186	186	186	186	186	186	186	186	186	186	186
NARWS - CRPL Quality Figures & Forecasts	175	176	177	178	179	180	181	182	183	184	185	186
NARWS - Comparison Graphs	175	176	177	178	179	180	181	182	183	184	185	186
NARWS - Graphs of Useful Frequency Ranges	175	176	177	178	179	180	181	182	183	184	185	186
NPRWS - CRPL Quality Figures & Forecasts	175	176	177	178	179	180	181	182	183	184	185	186
NPRWS - Comparison Graphs	175	176	177	178	179	180	181	182	183	184	185	186
Alert and SWI Decisions	174	175	176	177	178	179	180	181	182	183	184	185
Cosmic Ray Neutron Counts (Deep River)	195	195	195	195	195	195	195	195	195	195	195	195

INDEX FOR 1960-1961 DATA PUBLISHED IN CRPL-F Part B

	1960 Jan	Feb	Mar	Apr	May	Jun	Jul	Aug	Sep	Oct	Nov	Dec	1961 Jan	Feb	Mar	Apr	May	Jun	Jul	Aug	Sep	Oct	Nov	Dec
American Relative Sunspot Numbers R_A'	187	188	189	190	191	192	193	194	195	196	197	198	199	200	201	202	203	204	205	206	207	208	209	210
Zurich Provisional Relative Sunspot Number R_Z	186	187	188	189	190	191	192	193	194	195	196	197	198	199	200	201	202	203	204	205	206	207	208	209
Zurich Final Sunspot Numbers R_Z	199	199	199	199	199	199	199	199	199	199	199	199	211	211	211	211	211	211	211	211	211	211	211	211
Mt. Wilson Magnetic Characteristics of Sunspots																								
2800 Mc-Daily Values of Solar Flux (Ottawa)	186	187	188	189	190	191	192	193	194	195	196	197	198	199	200	201	202	203	204	205	206	207	208	209
Calcium Plage and Sunspot Regions	186	187	188	189	190	191	192	193	194	195	196	197	198	199	200	201	202	203	204	205	206	207	208	209
Coronal Line Emission Indices - Provisional	186	187	188	189	190	191	192	193	195	196	196	197	198	199	200	201	202	203	205	205	207	207	208	209
- Final	189	189	189	193	193	193	196	196	196	199	199	199	204	204	204	205	205	205	208	208	208	212	212	212
Optical Observations Flares	186	187	188	189	190	191	192	193	194	195	196	197	198	199	200	201	202	203	204	205	206	207	208	209
	189	190	191	192	193	194	195	196	197	198	199	200	201	202	203	204	205	206	207	208	210-	210	211	212
	191	191	194	194	201	195	201	201	201	199	201	201	208	208	208	208	208		208					
	194	194				201				201														
		196																						
Flare Patrol Observations	186	187	188	189	190	191	192	193	194	195	196	197	198	199	200	201	202	203	204	205	206	207	208	209
	189	190	191	192	193	194	195	196	197	198	199	200	201	202	203	204	205	206	207	208	210	210	211	212
	191	191			202	202	202	202	202	202	202	202	208	208	208	208	208		208					
Subflares	187	188	189	190	191	192	193	194	195	196	197	198	199	200	201	202	203	204	205	206	207	208	209	210
Ionospheric Effects (SWF)	187	188	189	190	191	192	193	194	195	196	197	198	199	200	201	202	203	204	207	206	207	208	209	210
(SCNA-SEA-Bursts)	188	189	189	190	191	192	193	194	195	196	197	198	199	200	201	202	203	204	205	206	207	208	209	210
(SPA)																		204	205	206	207	208	209	210
2800 Mc-Outstanding Occurrences (Ottawa)	186	187	188	189	190	191	192	193	194	195	196	197	198	199	200	201	202	203	204	205	206	207	208	209
																			206		209		209	
2800 Mc-Hours of Observation (Ottawa)	188	188	188	191	191	191	194	194	194	197	197	197	200	200	200	203	203	203	206	206	206	209	209	209
450-1000 Mc - (Owens Valley)											197	197	198	201	202	202	202	203	207	207	207	207		
											198													
25-580, 2100-3900 Mc - (Fort Davis)	197	197	197	198	198	198	199	199	199	200	200	200	203	203	203	204	204	204	208	208	208	209	209	209
169 Mc-Interferometric Observations (Nançay)	186	187	188	189	190	191	192	193	194	195	196	197	198	200	201	201	202	203	204	205	206	207	208	209
108 Mc-Outstanding Occurrences (Boulder)	186	187	188	189	190	191	192	193	194	195*	196	197	198	199	200	201	202	203	204	205	206	207	208	209
7.6-41 Mc-(HAO-Boulder)															207	207	207	207	207	207	207	207	208	209
9.1 cm - (Stanford)				196	197	199	210	211	212	212	212			213	213									
Cosmic Ray Neutron Counts (Climax)									195	196	197	198	199	200	201	202	203	204	205	206	207	208	210	210
Cosmic Ray Neutron Counts (Deep River)	195	195	195	195	195	195	195	195	195	196	197	198	199	200	201	202	203	204	204	206	207	208	209	210
					205														205					
Geomagnetic Indices C, Kp, Ap, - Selected Days	187	188	189	190+	191	192	193	194	195	196	197	198	199	200	201	202	203	204	205	206	207	208	209	210
27-Day Charts of Kp Indices for Year	198	198	198	198	198	198	198	198	198	198	198	198	208	208	208	208	208	208	208	208	208	208	208	208
NARWS - CRPL Quality Figures & Forecasts	187	188	189	190	191	192	193	194	195	196	197	198	199	200	201	202	203	204	205	206	207	208	209	210
NARWS - Comparison Graphs	187	188	189	190	191	192	193	194	195	196	197	198	199	200	201	202	203	204	205	206	207	208	209	210
NPRWS - CRPL Quality Figures & Forecasts	187	188	189	190	191	192	193	194	195	196	197	198	199	200	201	202	203	204	205	206	207	208	209	210
NPRWS - Comparison Graphs	187	188	189	190	191	192	193	194	195	196	197	198	199	200	201	202	203	204	205	206	207	208	209	210
NARWS - Graphs of Useful Frequency Ranges	187	188	190	190	191	192	193	194	195	196	197	198	199	200	201	202	203	204	205	206	207	208	209	210
Alert and SWI Decisions	186	187	188	189	190	191	192	193	194	195	196	197	198	199	200	201	202	203	204	205	206	207	208	209

FOOTNOTES: +F190 also includes R, relative sunspot number and C9, magnetic index in 27-day diagram January 1959-April 1959.
*Data up to October 1960 for 167 Mc.
Additional optical observations flares, for June 1959 in F 200.
International Geophysical Calendar for 1962 in F 207

INDEX FOR 1962-1963 DATA PUBLISHED IN CRPL-F PART B

	1962 Jan	Feb	Mar	Apr	May	Jun	Jul	Aug	Sep	Oct	Nov	Dec
American Relative Sunspot Numbers R_A'	211	212	213	214	215	216	217	218	219	220	221	222
Zurich Provisional Relative Sunspot Number R_Z	210	211	212	213	214	215	216	217	218	219	220	221
Zurich Final Sunspot Numbers R_Z	223	223	223	223	223	223	223	223	223	223	223	223
2800 Mc-Daily Values of Solar Flux (Ottawa)	210	211	212	213	214	215	216	217	218	219	220	221
2800 Mc-Daily Values of Solar Flux (Final - Ottawa)	223	223	223	223	223	223	223	223	223	223	223	223
Mt. Wilson Magnetic Characteristics of Sunspots	210	211	212	213	214	215	216	217	218	219	220	221
Calcium Plage and Sunspot Regions	210	211	212	213	214	215	216	217	218	219	220	221
Coronal Line Emission Indices - Provisional	210	211	212	213	214	215	216	217	218	219	220	221
- Final	213	213	213	216	216	216	220	220	220	226	226	226
Optical Observations Flares	210	211	212	213	214	215	216	217	218	219	220	221
	213	214	215	216	217	218	219	220	221	222	223	224
Flare Patrol Observations	210	211	212	213	214	215	216	217	218	219	220	221
	213	214	215	216	217	218	219	220	221	222	223	224
Subflares	211	From here on subflares included with flares.										
Ionospheric Effects (SWF)	211	212	213	214	215	216	219	219	219	220	221	222
(SCNA-SEA-Bursts)	211	212	213	214	215	216	219	219	219	220	221	222
(SPA)	211	212	213	214	215	216	219	219	219	220	221	222
2800 Mc-Outstanding Occurrences (Ottawa)	210	211	212	213	214	215	216	217	218	219	220	221
2800 Mc-Hours of Observations (Ottawa)	212	212	212	215	215	215	218	218	218	221	221	221
25-580 (50-320 as of Jan 1963) (Fort Davis)	213	213	213	216	216	216	219	219	219	222	222	222
221 Mc-Interferometric Occurrences (Boeing-Seattle)	-	-	-	221	221	221	221	221	221	221	221	221
169 Mc-Interferometric Observations (Nançay)	210	211	212	213	214	215	216	217	219	219	220	221
108 Mc-Outstanding Occurrences (Boulder)	210	211	212	213	214	215	216	217	218	219	220	221
108 Mc-Hours of Observations (Boulder)	210	211	212	213	214	215	216	217	218	219	220	221
7.6-41 Mc - (HAO-Boulder)	210	211	212	213	214	215	216	217	218	219	220	221
9.1 cm (Stanford)				213	214	215	216	217	218	219	220	221
Cosmic Ray Neutron Counts (Climax)	211	212	213	214	215	216	217	218	219	220	221	222
Cosmic Ray Neutron Counts (Deep River)	211	212	213	214	223	223	223	223	223	223	223	222
Geomagnetic Indices C, Kp, Ap, - Selected Days	211	212	213	214	215	216	217	218	219	220	221	222
27-Day Charts of Kp Indices for Year	221	221	221	221	221	221	221	221	221	221	221	221
NARWS - CRPL Quality Figures & Forecasts	211	212	213	214	215	216	217	218	219	220	221	222
NARWS - Comparison Graphs	211	212	213	214	215	216	217	218	219	220	221	222
NPRWS - CRPL Quality Figures & Forecasts	211	212	213	214	215	216	217	218	219	220	221	222
NPRWS - Comparison Graphs	211	212	213	214	215	216	217	218	219	220	221	222
NARWS - Graphs of Useful Frequency Range	211	212	213	214	215	216	217	218	219	220	221	222
Alert and SWI Decisions	210	211	212	213	214	215	216	217	218	219	220	221

* Addenda to July SWF in 230 and to August SWF in 231.

	1963 Jan	Feb	Mar	Apr	May	Jun	Jul	Aug	Sept	Oct	Nov	Dec
American Relative Sunspot Numbers R_A'	223	224	225	226	227	228	229	230	231	232	233	234
Zurich Provisional Relative Sunspot Number R_Z	222	223	224	225	226	227	228	229	230	231	232	233
Zurich Final Sunspot Numbers R	235	235	235	235	235	235	235	235	235	235	235	235
2800 Mc/s-Daily Values of Solar Flux (Ottawa)	222	223	224	225	226	227	228	229	230	231	232	233
2800 Mc/s-Daily Values of Solar Flux (Final-Ottawa)	233	233	233	233	233	233	233	233	233	233	233	233
2800 Mc/s-Daily Values of Adjusted Solar Flux (ARO)												
Mt. Wilson Magnetic Characteristics of Sunspots	222	223	224	225	none	227	228	229	230	231	232	233
Calcium Plage and Sunspot Regions	222	223	224	225	226	227	228	229	230	231	232	233
Coronal Line Emission Indices - Provisional	222	223	224	225	226	227	228	229	230	231	232	233
- Final	226	226	226	228	228	228	231	231	231	234	234	234
Optical Observations Flares	222	223	224	225	226	227	228	229	230	231	232	233
	225	226	227	228	229	230	231	232	233	234	235	236
Flare Patrol Observations	222	223	224	225	226	227	228	229	230	231	232	233
	225	226	227	228	229	230	231	232	233	234	235	236
Solar X-Ray Radiation												
Ionospheric Effects - (SWF-ABS-SCNA-SEA-SPA-SES-SFD-Bursts)*	223	224	225	226	227	228	229*	230*	231*	232	233	234
26 Mc/s Riometer Events (South Pole) - Provisional									231	232	233	234
2800 Mc/s - Outstanding Occurrences (ARO-Ottawa)	222	223	224	225	226	227	228	229	230	231	232	233
2800 Mc/s - Hours of Observations (ARO-Ottawa)	224	224	224	227	227	227	230	230	230	233	233	233
223 Mc/s - Interferometric Occurrences (Boeing - Seattle)	222#	223#	224#	225#	229	229	229					
169 Mc/s - Interferometric Observations (Nancay)	222	223	224	225	226	227	228	229	230	231	232	233
108 Mc/s - Outstanding Occurrences (Boulder)	222	223	224	225	226	227	228	229	230	231	232	233
108 Mc/s - Hours of Observation (Boulder)	222	223	224	225	226	227	228	229	230	231	232	233
50 - 320 Mc/s - (Fort Davis)+	225	225	225	228	228	228	230	230	230	234	234	234
7.6-41 Mc - (HAO-Boulder)	222	223	224	225	226	227	228	229	230	231	232	233
9.1 cm (Stanford)	222	-	-	225	226	227	228	229	230	231	232	233
Cosmic Ray Neutron Counts (Climax)	223	224	225	226	227	228	229	230	231	232	234	234
Cosmic Ray Neutron Counts (Deep River)	223	224	225	226	227	228	229	230	231	232	233	234
Geomagnetic Indices C, Kp, Ap - Selected Days	223	224	225	226	227	228	229	230	231	232	233	234
27-Day Chart of Kp Indices for Year	233	233	233	233	233	233	233	233	233	233	233	233
27-Day Chart of C9 for Year	233	233	233	233	233	233	233	233	233	233	233	233
NARWS - CRPL Quality Figures & Forecasts	223	224	225	226	227	228	229	230	231	232	233	234
NARWS - Comparison Graphs	223	224	225	226	227	228	229	230	231	232	233	234
NPRWS - CRPL Quality Figures & Forecasts	223	224	225	226	227	228	229	230	231	232	233	234
NPRWS - Comparison Graphs	223	224	225	226	227	228	229	230	231	232	233	234
NARWS - Graphs of Useful Frequency Range	223	224	225	226	227	228	229	230	231	232	233	234
IQSY Alert Decisions**	222	223	224	225	226	227	228	229	230	231	232	233

* Addenda to July SWF in 230 and to August SWF in 231
\+ 25-580 Mc/s (Fort Davis) prior to January 1963
** Alert and SWI Decisions before November 1963
° Revisions to September Climax Monitor in 234
°° Addenda to Jan. Feb. and Mar. 1964 - Flares in 240 and 241
\# = 221 Mc/s before May 1963

Cosmic ray indices from Dallas super neutron monitor for January through September 1964 and from Churchill super neutron monitor for May through September 1964 were given in 243.

INDEX FOR 1964 DATA PUBLISHED IN CRPL-F PART B

	1964											
	Jan	Feb	Mar	Apr	May	Jun	Jul	Aug	Sep	Oct	Nov	Dec
American Relative Sunspot Numbers R_A	235	236	237	238	239	240	241	242	243	244	245	246
Zurich Provisional Relative Sunspot Number R_Z	234	235	236	237	238	239	240	241	242	243	244	245
Zurich Final Sunspot Numbers R_Z	247	247	247	247	247	247	247	247	247	247	247	247
2800 Mc/s-Daily Values of Solar Flux (Ottawa)	234	235	236	237	238	239	240	241	242	243	244	245
2800 Mc/s-Daily Values of Solar Flux (Final-Ottawa)	245	245	245	245	245	245	245	245	245	245	245	245
2800 Mc/s-Daily Values of Adjusted Solar Flux (ARO)	240	240	240	240	240	240	240	241	242	243	244	245
2800 Mc/s-Daily Values of Adjusted Solar Flux (Final-Ottawa)	245	245	245	245	245	245	245	245	245	245	245	245
Mt. Wilson Magnetic Characteristics of Sunspots	234	235	236	237	238	239	240	241	242	243	244	245
Calcium Plage and Sunspot Regions	234	235	236	237	238	239	240	241	242	243	244	245
Coronal Line Emission Indices - Provisional	234	235	236	237	238	239	240	241	242	243	244	245
- Final	237	237	237	240	240	240	243	243	243	248	248	248
Optical Observations Flares	234*	235*	236*	237	238	239	240	241	242	243	244	245
	237	238	239	240	241	242	243	244	245	246	248	248
Flare Patrol Observations	234	235	236	237	238	239	240	241	242	243	244	245
	237	238	239	240	241	242	243	244	245	246	248	248
Solar X-Ray Radiation	243	247	247	241	241	241	244	244	245	245		
Solar X-Ray Radiation (Revised)				249	255	264	266	266				
Ionospheric Effects - (SWF-SCNA-SEA-SPA-SES-SFD-Bursts)	235	236	237	238	239	240	241	242	243	244	245	246
26 Mc/s Riometer Events (South Pole) - Provisional	235	236	237	238	239	240	241	242	243	244	245	246
30 Mc/s Riometer Events (Frobisher Bay) - Final												
30 Mc/s Riometer Events (Great Whale River)												
10700, 2700, 960, 328 Mc/s - Solar Noise Observations (Pennsylvania State University)							252	252	252	252	252	252
2800 Mc/s - Outstanding Occurrences (ARO-Ottawa)	234	235	236	237	238	239	240	241	242	243	244	245
2800 Mc/s - Hours of Observations (ARO-Ottawa)	236	236	236	239	239	239	242	242	242	245	245	245
223 Mc/s - Interferometric Occurrences (Boeing - Seattle)												
169 Mc/s - Interferometric Observations (Nançay)	234	235	236	237	238	239	240	241	242	243	244	245
108 Mc/s - Outstanding Occurrences (Boulder)	234	235	236	237	238	239	240	241	242	243	244	245
108 Mc/s - Hours of Observation (Boulder)	234	235	236	237	238	239	240	241	242	243	244	245
107 Mc/s - Outstanding Occurrences (Haleakala)												
50 - 320 Mc/s - (Fort Davis)+	237	237	237	240	240	240	243	243	243	246	246	246
7.6-41 Mc/s-(HAO - University of Colorado - Boulder)	234	235	236	237	238	239	240	241	242	243	244	245
9.1 cm Spectroheliograms (Stanford)	234	235	236	237	238	239	240	241	242	243	244	245
21 cm Spectroheliograms (Fleurs)												250
21 cm Solar Scans (Fleurs)												
Cosmic Ray Neutron Counts (Deep River)	235	236	237	238	239	240	241	242	243	244	245	246
Cosmic Ray Neutron Counts (Churchill)					245	243	243	243	243	244	245	246
Cosmic Ray Neutron Counts (Climax)	235	236	237	238	239	240	241	242	243	244	245	246
Cosmic Ray Neutron Counts (Dallas)	243	243	243	243	243	243	243	243	243	244	245	246
Geomagnetic Indices C, Kp, Ap - Selected Days	235	236	237	238	239	240	241	242	243	244	245	246
27-Day Chart of Kp Indices for Year	245	245	245	245	245	245	245	245	245	245	245	245
27-Day Chart of C9 for Year	245	245	245	245	245	245	245	245	245	245	245	245
NARWS - CRPL Quality Figures and Forecasts	235	236	237	238	239	240	241	242	243	244	245	246
NPRWS - CRPL Quality Figures and Forecasts	235	236	237	238	239	240	241	242	243	244		
High Latitude - CRPL Quality Figures and Forecasts											245	246
High Latitude - Comparison Graphs											245	246
NARWS - Comparison Graphs	235	236	237	238	239	240	241	242	243	244	245	246
NPRWS - Comparison Graphs	235	236	237	238	239	240	241	242	243	244		
NARWS - Graphs of Useful Frequency Range	235	236	237	238	239	240	241	242	243	244	245	246
IQSY Alert Decisions	234	235	236	237	238	239	240	241	242	243	244	245

FOOTNOTES: *Addenda to Jan. Feb. and Mar. 1964 - Flares in 240 and 241
+25- 320 Mc/s (Fort Davis) beginning April 1965
X-Ray (SR-3 and Injun 1) June-Dec. 1961 in 249
X-Ray (Vela) October 18-31, 1963 in 249
Radar Meteor Indices were published in 246 and 251

INDEX FOR 1965 DATA PUBLISHED IN CRPL-F PART B

1965

	Jan	Feb	Mar	Apr	May	Jun	July	Aug	Sep	Oct	Nov	Dec
American Relative Sunspot Numbers R_A	247	248	249	250	251	252	253	254	255	256	257	257
Zürich Provisional Relative Sunspot Numbers R_Z	246	247	248	249	250	251	252	253	254	255	256	257
Zürich Final Sunspot Numbers R_Z	258	258	258	258	258	258	258	258	258	258	258	258
2800 Mc/s-Daily Values of Solar Flux (Ottawa)	246	247	248	249	250	251	252	253	254	255	256	257
2800 Mc/s-Daily Values of Solar Flux (Final-Ottawa)	257	257	257	257	257	257	257	257	257	257	257	257
2800 Mc/s-Daily Values of Adjusted Solar Flux (ARO)	246	247	248	249	250	251	252	253	254	255	256	257
2800 Mc/s-Daily Values of Adjusted Solar Flux (Final-Ottawa)	257	257	257	257	257	257	257	257	257	257	257	257
Mt. Wilson Magnetic Characteristics of Sunspots	246	247	248	249	---	251	252	253	254	255	256	257
Mt. Wilson Magnetograms												
Calcium Plage and Sunspot Regions	246	247	248	249	250	251	252	253	254	255	256	257
Coronal Line Emission Indices - Provisional	247	248	248	249	250	251	252	253	---	256	257	257
- Final	249	249	249	252	252	252	256	256	256	258	258	258
Optical Observations Flares	246	247	248	249	250	251	252	253	254	255	256	257
	249	250	251	252	253	255	255	256	257	258	259	260
Optical Observations Flares (Addenda)												
Flare Patrol Observations	246	247	248	249	250	251	252	253	254	255	256	257
	249	250	251	252	253	255	255	256	257	258	259	260
Solar X-Ray Radiation (NRL)			279	279	279	279	279	279	279	279	276	276
Solar X-Ray Radiation (Aberdeen, S. Dakota)												
Solar X-Ray Radiation (France)												
Solar X-Ray Radiation (ESSA-Boulder)												270
Ionospheric Effects - (SWF-SCNA-SEA-SPA-SES-SFD-Bursts)	247	248	249	250	251	252	253	254	255	256	257	258
30 Mc/s Riometer Events (Frobisher Bay)	247	248	249	250	251							
30 Mc/s Riometer Events (Great Whale River)						252	253	254	255	256	257	258
10700, 2700, 960, 328 Mc/s - Outstanding Occurrences (Pennsylvania State University)	252	252	252	256	256	256	263	263	263	263	263	263
8800, 4995, 2695, 1415 and 606 Mc/s Outstanding Occurrences (AFCRL, Sagamore Hill)												
2800 Mc/s - Outstanding Occurrences (ARO-Ottawa)	246	247	248	249	250	251	252	253	254	255	256	257
2800 Mc/s - Hours of Observations (ARO-Ottawa)	248	248	248	251	251	251	254	254	254	257	257	257
486 Mc/s - Outstanding Occurrences (Washington State Univ.)												
223 Mc/s - Interferometric Occurrences (Boeing - Seattle)					251	252	253	253	254	255	256	
408 Mc/s - Interferometric Observations (Nancay)											257	257
169 Mc/s - Interferometric Observations (Nancay)	246	---	---	---	---	---	---	253	254	255	257	257
108 Mc/s - Outstanding Occurrences (Boulder)	246	247	248	249	250	251	252	253	254	255	256	257
108 Mc/s - Hours of Observation (Boulder)	246	247	248	249	250	251	252	253	254	255	256	257
107 Mc/s - Outstanding Occurrences (Haleakala)						252	253	253	254	255	256	257
25 - 320 Mc/s - (Fort Davis)+	249	249	249	252	252	252	255	255	255	258	258	258
7.6-41 Mc/s - (HAO - University of Colorado - Boulder)	246	247	248	249	250	251	252	253	254	255	256	257
9.1 cm Spectroheliograms (Stanford)	246	247	248	249	250	251	252	253	254	255	256	257
21 cm Spectroheliograms (Fleurs)	250	250	254	254	257	257	257	259	260	263	263	263
21 cm Solar Scans (Fleurs)										255	256	257
43 cm Solar Scans (Fleurs)												
Cosmic Ray Neutron Counts (Deep River)	247	248	249	250	251	252	253	254	255	256	257	258
Cosmic Ray Neutron Counts (Alert)												
Cosmic Ray Neutron Counts (Churchill)	247	248	249	250	251	252	253	254	255	256	257	258
Cosmic Ray Neutron Counts (Climax)	247	248	249	250	251	252	253	254	255	256	257	258
Cosmic Ray Neutron Counts (Dallas)	247	248	249	250	251	252	253	254	255	256	257	258
Geomagnetic Indices Ci, Cp, Kp, Ap - Selected Days	247	248	249	250	251	252	253	254	255	256	257	258
Principal Magnetic Storms												
Sudden Commencement and Solar Flare Effects												
27-Day Chart of Kp Indices for Year	258	258	258	258	258	258	258	258	258	258	258	258
27-Day Chart of C9 for Year	258	258	258	258	258	258	258	258	258	258	258	258
NARWS - CRPL Quality Figures and Forecasts	247	248	249	250	251	252	253	254	255	256	257	258
NPRWS - CRPL Quality Figures and Forecasts	247	248	249	250	251	252	253	254	255	256	257	258
High Latitude - CRPL Quality Figures and Forecasts	247	248	249	250	251	252	253	254	255	256	257	258
High Latitude - Comparison Graphs	247	248	249	250	251	252	253	254	255	256	257	258
NARWS - Comparison Graphs	247	248	249	250	251	252	253	254	255	256	257	258
NPRWS - Comparison Graphs												
NARWS - Graphs of Useful Frequency Range	247	248	249	250	251	252	253	254	255	256	257	258
IQSY/IUWDS Alert Decisions	246	247	248	249	250	251	252	253	254	255	256	257

NOTES: +50 -320 Mc/s (Fort Davis) before April 1965
X-Ray (SR-3 and Injun 1) June-Dec. 1961 in 249
X-Ray (Vela) October 18-31, 1963 in 249
Radar Meteor Indices were published in 246 and 251

INDEX FOR 1966-1967 DATA PUBLISHED IN IER-FB

	1966 Jan	Feb	Mar	Apr	May	Jun	Jul	Aug	Sep	Oct	Nov	Dec	1967 Jan	Feb	Mar	Apr	May	Jun	Jul	Aug	Sep	Oct	Nov	Dec	1968 Jan
American Relative Sunspot Numbers R_A	258	259	260	261	262	263	264	265	266	267	268	269	270	271	272	273	274	275	276	277	278	279	280	281	282
Zürich Provisional Relative Sunspot Numbers R_Z	258	259	260	261	262	263	264	265	266	267	268	269	270	271	272	273	274	275	276	277	278	279	280	281	282
Zürich Final Sunspot Numbers R_Z	271	271	271	271	271	271	271	271	271	271	271	271	282	282	282	282	282	282	282	282	282	282	282	282	
2800 MHz - Daily Values of Solar Flux (Ottawa)	258	259	260	261	262	263	264	265	266	267	268	269	270	271	272	273	274	275	276	277	278	279	280	281	282
2800 MHz - Daily Values of Solar Flux (Final-Ottawa)	269	269	269	269	269	269	269	269	269	269	269	269													
2800 MHz - Daily Values of Adjusted Solar Flux (ARO)	258	259	260	261	262	263	264	265	266	267	268	269	270	271	272	273	274	275	276	277	278	279	280	281	282
2800 MHz - Daily Values of Adjusted Solar Flux (Final-Ottawa)	269	269	269	269	269	269	269	269	269	269	269	269													
8800, 4995, 2695, 1415, 606 MHz Adjusted Solar Flux (AFCRL)													270	271	272	273	274	275	276	277	278	279	280	281	282
Mt. Wilson Magnetic Characteristics of Sunspots	258	259	260	261	262	263	264	265	266	267	268	269	270	271	272	273	274	275	276	277	278	279	280	281	282
Mt. Wilson Magnetograms									269	269	269	270	271	272	273	274	275	276	277	278	279	280	281	282	
Hα (Sacramento-Peak)													271	272	273	274	275	276	277	278	279	280	281	282	
Sunspots (Boulder)													271	272	273	274	275	276	277	278	279	280	281	282	
Calcium Plage Maps (McMath-Hulbert)													271	272	273	274	275	276	277	278	279	280	281	282	
Calcium Plage and Sunspot Regions	258	259	260	261	262	263	264	265	266	267	268	269	270	271	272	273	274	275	276	277	278	279	280	281	282
Coronal Line Emission Indices	261	261	261	264	264	264	267	267	267	270	270	270	271	272	273	275	275	276	277	278	279	280	282	282	
Optical Observations Flares	258	259	260	261	262	263	264	265	266	267	268	269	270	271	272	273	274	275	276	277	278	279	280	281	282
Optical Observations Flares[1]	261	262	263	264	265	266	267	268	269	272	273	274	275	276	277	278	279	280	281	282					
Optical Observations Flares (Addenda)		266		266&268	266			270	271						278									
Flare Patrol Observations	258	259	260	261	262	263	264	265	266	267	268	269	270	271	272	273	274	275	276	277	278	279	280	281	282
Flare Patrol Observations	261	262	263	264	265	266	267	268&270	269&271	272	273	274	275	276	277	278	279	280	281	282					
Solar X-Ray Radiation (NRL)[2]	276	276	264	276	276	264	265	267	267	269	269	269	271	272	273	274	275	276	277	278	279	280	281	282	
X-Ray Graphs (NRL)								279		272	273	274	275	276	277	278	279	280	281						
Solar X-Ray Radiation (Aberdeen, S. Dakota)	261	261	261	261	262	263	264	265	266	---	272	---	---	272	273	274	---	276	277	---	279	280			
Solar X-Ray Radiation (France)				267	267																				
Solar X-Ray Radiation (ESSA-Boulder)	270	270	270	270	271	271	271	271	271	271	271	271	271	272	273	274	275	---	---	278	279	280	281		
X-Ray (University of Iowa)							275	275	275	275	275	277	278	278	278	280	280	281	281						
X-Ray (McMath-Hulbert)															278	279	279	280	281	282					
Solar Wind Velocities (Ames Research Center)																							281	281	282
Ionospheric Effects (SWF-SCNA-SEA-SPA-SES-SFD-Bursts)[3]	259	260	261	262	263	264	265	266	267	268	269	270	271	272	273	274	275	276	277	278	279	280	281	282	
30 MHz Riometer Events (Great Whale River)	259	260	261	262	263	264	265	266	267	268	269	270	271	272	---	---	---	---	---	---	---	---	---	---	
30 MHz Riometer Events (South Pole)															273	274	275	276	277	278	279	280	281	---	
10700, 2700, 960, 328 MHz - Outstanding Occurrences (Pennsylvania State University)	258	259	260	261	262	263	264	265	266	267	268	269	270	271	272	273	274	275	276	277	278	279	280	281	282
8800, 4995, 2695, 1415, and 606 MHz Outstanding Occurrences (AFCRL, Sagamore Hill)[6]	260	260	260	261	262	263	264	265	266	267	268	269	270	271	272	273	274	275	276	277	278	279	280	281	282
7000 MHz (Sao Paulo)																							280	281	282
2800 MHz - Outstanding Occurrences (ARO-Ottawa)	258	259	260	261	262	263	264	265	266	267	268	269	270	271	272	273	274	275	276	277	278	279	280	281	282
486 MHz - Outstanding Occurrences (Washington State Univ.)							264	265	266	267	268	269	270	271	272	273	274	275	276	277	278	279	280	281	
408 MHz - Outstanding Occurrences (San Miguel)																						279	280	281	282
408 MHz - Interferometric Observations (Nancay)	258	259	260	261	262	264	264	265	266	267	268	269	270	271	272	273	275	275	276	277	279	279	280	281	282
169 MHz - Interferometric Observations (Nancay)	258	259	260	261	262	264	264	265	266	267	268	269	270	271	272	273	---	---	277	277	279	279	280		
184 MHz - Outstanding Occurrences (Boulder)[4]	258	259	260	261	262	263	---	---	---	---	---	---	---	---	272	273	274	275	276	277	278	279	280	281	282
107 MHz - Outstanding Occurrences (Haleakala)	258	---	261	---	---	---	---	---	---	---	---	---	---	---	---	---	---	---	---	---	---	---	---	---	---
18 MHz - Bursts (Boulder)																								281	282
18 MHz - Bursts (McMath)																									282
10-580 MHz - (Fort Davis)[5]	261	261	261	264	264	264	267	267	267	270	270	270	277	277	277	277	277	277	277	278	279	280	281	282	
10-210 MHz - (Culgoora)													277	277	277	277	277	277	277	278	279	280	281	282	
7.6-41 MHz - University of Colorado - Boulder)	258	259	260	261	262	263	264	265	266	267	268	269	270	271	272	273	274	275	276	278	279	280	281	282	
19-41 MHz - (AFCRL, Sagamore Hill)																									
9.1 cm Spectroheliograms (Stanford)	258	259	260	261	262	263	264	265	266	267	268	269	271	272	273	274	275	276	277	278	279	280	281	282	
21 cm Spectroheliograms (Fleurs)	263	263	263	266	266	266	267	267	267	268	---	269	271	272	273	274	275	276	277	278	---	280	281	282	
21 cm Solar Scans (Fleurs)	258	259	260	261	262	263	264	265	266	267	268	269	270	271	272	273	274	275	276	277	278	280	280	281	282
43 cm Solar Scans (Fleurs)				261	262	263	264	265	266	267	268	269	270	271	272	273	274	275	276	277	278	280	280	281	282
Cosmic Ray Neutron Counts (Deep River)	259	260	261	262	263	264	265	266	267	268	269	270	271	272	273	274	275	276	277	278	279	280	281	282	
Cosmic Ray Neutron Counts (Alert)							265	266	267	268	269	270	271	272	273	274	275	276	277	278	279	280	281	282	
Cosmic Ray Neutron Counts (Churchill)	259	260	261	274	274	274	274	274	274	274	274	274												282	
Cosmic Ray Neutron Counts (Climax)	259	260	261	262	263	264	265	266	267	268	269	270	271	272	273	274	275	276	277	278	279	280	281	282	
Cosmic Ray Neutron Counts (Dallas)	259	260	261	275	275	275	275	275	275													280	281	282	
Solar Protons (Satellite)																	282	282	282	282					
Solar Proton Events (Riometer)																									
Geomagnetic Indices Ci, Cp, Kp, Ap - Selected Days	259	260	261	262	263	264	265	266	267	268	269	270	271	272	273	274	275	276	277	278	279	280	281	282	
Principal Magnetic Storms							270	270	270	270	270	270	271	272	273	274	275	276	277	278	279	280	281	282	
Sudden Commencement and Solar Flare Effects	270	270	270	270	270	270	270	270	270	273	273	273	277	277	277	280	280	280							
27-Day Chart of Kp Indices for Year	270	270	270	270	270	270	270	270	270	270	270	270	282	282	282	282	282	282	282	282	282	282	282	282	
27-Day Chart of C9 for Year	270	270	270	270	270	270	270	270	270	270	270	270	282	282	282	282	282	282	282	282	282	282	282	282	
High Latitude Quality Figures and Forecasts	259	260	261	262	263	264	265	266	267	268	269	270	271	272	273	274	275	276	277	278	279	280	281	282	
High Latitude Comparison Graphs	259	260	261	262	263	264	265	266	267	268	269	270	271	272	273	274	275	276	277	278	279	280	281	282	
Graphs of Transmission Frequency Range	259	260	261	262	263	264	265	266	267	268	269	270	271	272	273	274	275	276	277	278	279	280	281	282	
IUWDS Alert Decisions	258	259	260	261	262	263	264	265	266	267	268	269	270	271	272	273	274	275	276	277	278	279	280	281	282

NOTES: 1. Includes Standardized Flare Data beginning September 1966.
2. March-October 1965 in FB-279, November-December 1965 in FB-276.
3. No 18 MHz Bursts reported beginning December 1966; with outstanding occurrences Nov.-Dec. 1967.
4. 108 MHz (Boulder) in 1966.
5. 25-320 MHz (Fort Davis) in 1966.
6. Also 15400 MHz beginning in FB-280.

B = +0°
N
B = −0°
N

B = +1°
N
B = −1°
N

B = +2°
N
B = −2°
N

B = +3°
N
B = −3°
N

B = +4°
N
B = −4°
N

B = +5°
N
B = −5°
N

B = +6°
N
B = −6°
N

B = +7°
N
B = −7°
N